AMERICAN SOCIETY FOR MICROBIOLOGY | mBio®

RESEARCH ARTICLE

HIV-1 Vpu Promotes Phagocytosis of Infected CD4$^+$ T Cells by Macrophages through Downregulation of CD47

Lijun Cong,[a] Scott M. Sugden,[a] Pascal Leclair,[b] Chinten James Lim,[b] Tram N. Q. Pham,[a] Éric A. Cohen[a,c]

[a]Laboratory of Human Retrovirology, Institut de Recherches Cliniques de Montréal (IRCM), Montreal, Quebec, Canada
[b]Department of Pediatrics, University of British Columbia, Vancouver, British Columbia, Canada
[c]Department of Microbiology, Infectiology and Immunology, Faculty of Medicine, Université de Montréal, Montreal, Quebec, Canada

ABSTRACT Human immunodeficiency virus (HIV) remodels the cell surface of infected cells to facilitate viral dissemination and promote immune evasion. The membrane-associated viral protein U (Vpu) accessory protein encoded by HIV-1 plays a key role in this process by altering cell surface levels of multiple host proteins. Using an unbiased quantitative plasma membrane profiling approach, we previously identified CD47 as a putative host target downregulated by Vpu. CD47 is a ubiquitously expressed cell surface protein that interacts with the myeloid cell inhibitory receptor signal regulatory protein-alpha (SIRPα) to deliver a "don't-eat-me" signal, thus protecting cells from phagocytosis. In this study, we investigate whether CD47 modulation by HIV-1 Vpu might promote the susceptibility of macrophages to viral infection via phagocytosis of infected CD4$^+$ T cells. Indeed, we find that Vpu downregulates CD47 expression on infected CD4$^+$ T cells, leading to enhanced capture and phagocytosis by macrophages. We further provide evidence that this Vpu-dependent process allows a C-C chemokine receptor type 5 (CCR5)-tropic transmitted/founder (T/F) virus, which otherwise poorly infects macrophages in its cell-free form, to efficiently infect macrophages. Importantly, we show that HIV-1-infected cells expressing a Vpu-resistant CD47 mutant are less prone to infecting macrophages through phagocytosis. Mechanistically, Vpu forms a physical complex with CD47 through its transmembrane domain and targets the latter for lysosomal degradation. These results reveal a novel role of Vpu in modulating macrophage infection, which has important implications for HIV-1 transmission in early stages of infection and the establishment of viral reservoir.

IMPORTANCE Macrophages play critical roles in human immunodeficiency virus (HIV) transmission, viral spread early in infection, and as a reservoir of virus. Selective capture and engulfment of HIV-1-infected T cells was shown to drive efficient macrophage infection, suggesting that this mechanism represents an important mode of infection notably for weakly macrophage-tropic T/F viruses. In this study, we provide insight into the signals that regulate this process. We show that the HIV-1 accessory protein viral protein U (Vpu) downregulates cell surface levels of CD47, a host protein that interacts with the inhibitory receptor signal regulatory protein-alpha (SIRPα), to deliver a "don't-eat-me" signal to macrophages. This allows for enhanced capture and phagocytosis of infected T cells by macrophages, ultimately leading to their productive infection even with transmitted/founder (T/F) virus. These findings provide new insights into the mechanisms governing the intercellular transmission of HIV-1 to macrophages with implications for the establishment of the macrophage reservoir and early HIV-1 dissemination *in vivo*.

KEYWORDS CD47, HIV, HIV dissemination, HIV infection, Vpu, macrophage reservoir, macrophages, phagocytosis

Citation Cong L, Sugden SM, Leclair P, Lim CJ, Pham TNQ, Cohen ÉA. 2021. HIV-1 Vpu promotes phagocytosis of infected CD4$^+$ T cells by macrophages through downregulation of CD47. mBio 12:e01920-21. https://doi.org/10.1128/mBio.01920-21.

Editor Vinayaka R. Prasad, Albert Einstein College of Medicine

Address correspondence to Éric A. Cohen, eric.cohen@ircm.qc.ca.

Received 29 June 2021
Accepted 23 July 2021
Published 24 August 2021

The viral protein U (Vpu) is a membrane-associated accessory protein encoded by human immunodeficiency virus type 1 (HIV-1) and related simian immunodeficiency viruses (SIVs) but not by HIV-2. Consistent with the roles of HIV-1 accessory proteins in targeting cellular restriction factors to favor immune evasion and viral dissemination, Vpu counteracts many host proteins, including BST2/tetherin to promote efficient viral particle release (1, 2) and CD4 to avoid superinfection and subsequent premature cell death (3). The downregulation of both CD4 and BST2 also protects HIV-1-infected $CD4^+$ T cells from antibody-mediated cellular cytotoxicity (ADCC) (4). Given the contribution of Vpu toward HIV pathogenesis, partly through targeting BST2 and CD4, there is a continuing interest in identifying additional Vpu targets. To date, a diverse list of host factors has been identified, including CD1d, NK-T-B antigen (NTB-A)/Signaling Lymphocytic Activation Molecule Family member 6 (SLAMF6), poliovirus receptor (PVR)/CD155, C-C motif chemokine receptor 7 (CCR7), CD62L, sodium-coupled neutral amino acid transporter 1 (SNAT1) (5), intercellular adhesion molecule 1 and 3 (ICAM1/3) (6), CD99, proteolipid protein 2 (PLP2) (7), P-selectin glycoprotein ligand-1 (PSGL-1) (8), T cell immunoglobulin and mucin domain-containing protein 3 (Tim-3) (9), and likely more yet to be discovered. Indeed, using a stable isotope labeling of amino acids in cell culture (SILAC)-based proteomic approach, we and others previously identified CD47 as a potential target that is downmodulated by Vpu (6, 10).

CD47, also known as integrin-associated protein (IAP), is a ubiquitously expressed type I transmembrane protein (11) that serves as a ligand of the signal regulatory protein-alpha (SIRPα, or CD172a), an inhibitory receptor mainly expressed on myeloid cells, such as macrophages and dendritic cells (DCs) (12, 13), but also on cytolytic T lymphocytes (14). The interaction between these two proteins results in a "don't-eat-me" signal that inhibits phagocytosis of target cells expressing CD47 by macrophages and DCs, thus providing an important regulatory switch for the phagocytic function of these cells.

Macrophages make up a heterogenous population of immune cells that play important roles in tissue homeostasis and host defense against pathogens partly through their phagocytic function (15). They are increasingly recognized as important cellular targets of HIV-1 infection (16, 17). Indeed, given their relative lengthy life span and unique ability to resist HIV-1 cytopathic effects and $CD8^+$ T cell-mediated killing (18, 19), macrophages are thought to be an important viral sanctuary and vector for HIV-1 dissemination as well as a potential viral reservoir during antiretroviral therapy (ART) (20–23). Macrophages are among the early targets of HIV-1 infection given their proximity to the portal of viral entry, commonly the mucosal tissue (21, 24). They express the CD4 receptor and both chemokine coreceptors C-X-C motif chemokine receptor 4 (CXCR4) and CCR5. While macrophage-tropic (M-tropic) viruses mainly use CCR5 as a coreceptor, they are paradoxically mostly isolated from brain tissues of AIDS patients at late stages of infection (17, 25). Yet, infected tissue macrophages can be detected at all stages of disease (26), and transmitted/founder (T/F) viruses that initiate infection as well as interindividual transmission are weakly M-tropic (27). It is therefore crucial to understand the mechanisms by which macrophages become infected during the early phase of infection. In this regard, it has been reported that macrophages capture SIV- or HIV-1-infected T cells, retain infectious particles in a nondegradative compartment and ultimately become infected (28–30). As well, proinflammatory cytokines secreted shortly after infection (31) may activate macrophages and enhance the phagocytosis of infected $CD4^+$ T cells in proximity *in vivo*.

Putting our observation in this context, we investigated whether Vpu-mediated CD47 downregulation would facilitate macrophage infection by promoting phagocytosis of HIV-1-infected $CD4^+$ T cells. In the current study, we report that Vpu downregulates CD47 from the surface of infected $CD4^+$ T cells. We also show that CD47 modulation by Vpu promotes enhanced capture and phagocytosis of T cells by monocyte-derived macrophages (MDMs), which ultimately leads to productive infection of MDMs. In addition, our findings uncover that through this process, a T/F virus could efficiently infect MDMs, revealing a possible model for macrophage infection at early

stages of infection. Importantly, mechanistic studies reveal that Vpu depletes CD47 via a process that requires its transmembrane domain (TMD) for binding CD47 as well as the DSGNES diserine motif and the EXXXLV trafficking motif for targeting CD47 to lysosome-dependent degradation.

RESULTS

Vpu downregulates CD47 from the surface of HIV-1-infected CD4$^+$ T cells. To verify the expression profile of CD47 in the context of HIV-1 infection, we first examined the effect of Vpu on CD47 surface expression levels in HIV-1-infected SupT1 cells that do not express BST2 (32). Given that both BST2 and CD47 localize to lipid rafts at the cell surface (12, 33) and, as such, might be part of supramolecular protein complexes, the use of SupT1 cells would indicate whether the effect of Vpu on CD47 was independent from BST2 downmodulation by Vpu. To this end, SupT1 cells were infected with the CXCR4 (X4)-tropic green fluorescent protein (GFP)-marked NL4-3 HIV-1 (NL4-3) expressing (wild-type [WT]) or lacking Vpu (dU), and surface expression of CD47 was measured by flow cytometry at 48 h postinfection (hpi). Infection with WT HIV-1 resulted in an ~30% decrease in surface CD47 levels on infected cells compared to bystander GFP cells or cells infected with dU HIV-1, suggesting that modulation of CD47 by Vpu did not involve BST2 (Fig. 1). This downregulation of CD47 was also observed to various extents in primary CD4$^+$ T cells infected with either NL4-3, CCR5 (R5)-tropic NL 4-3.ADA.IRES.GFP (NL 4-3 ADA), or R5-tropic T/F WITO virus expressing Vpu (16% to 24% downregulation; average of $n = 4$). Importantly, no such modulation in CD47 expression was noted in cells infected with the respective dU derivatives of these viruses (Fig. 1), further confirming a Vpu-dependent downregulation of CD47 during HIV infection of primary CD4$^+$ T cells.

CD47 is reported to undergo posttranslational pyroglutamate modification at the SIRPα binding site by the glutaminyl-peptide cyclotransferase-like protein (QPCTL), a modification that is thought to positively regulate the CD47/SIRPα axis by enhancing SIRPα binding (34). Since CD47 surface expression was detected using anti-human CD47 monoclonal antibody (MAb) clone CC2C6, which specifically recognizes the pyroglutamate of CD47, we next assessed whether Vpu targeting of CD47 is dependent or independent of the pyroglutamate epitope. Using the anti-human CD47 MAb clone B6H12 that recognizes all forms of CD47 at the cell surface, we found that the extent of Vpu-mediated downregulation of CD47 (~40%) was comparable to that detected with the CC2C6 MAb in infected Jurkat E6.1 cells (Fig. S1 in the supplemental material). Together, these data show that Vpu downregulates all forms of CD47 from the surface of HIV-1-infected CD4$^+$ T cells.

Vpu-mediated CD47 downregulation enhances capture and phagocytosis of infected T cells by MDMs. CD47 is known to function as a marker of "self" that protects healthy cells from being engulfed by macrophages. Accordingly, hematopoietic cells lacking CD47 are efficiently cleared by macrophages (35). Therefore, we hypothesized that Vpu-mediated downregulation of CD47 modulates the capture and phagocytosis of HIV-1-infected T cells by MDMs. To test this, we generated a CD47 knockout (CD47KO) Jurkat E6.1 cell line (Fig. S2A and B). First, target Jurkat cells (CD47-expressing control cells and CD47KO cells) were infected with NL 4-3 ADA (WT or dU) for 48 h and were then labeled with carboxyfluorescein succinimidyl ester (CFSE) and cocultured with MDMs for 2 h to assess the capture of labeled T cells by CD11b-expressing macrophages using flow cytometry (Fig. 2A). As shown in Fig. 2B, we observed a significantly higher frequency of CD11b$^+$/CFSE$^+$ MDMs upon coculture with WT-infected CD47-expressing Jurkat cells (~12%; average of $n = 4$) than upon coculture with mock- or dU-infected Jurkat cells (~7.5 or 8.8%; respectively, average of $n = 4$). When MDMs were cocultured with CD47KO Jurkat cells, there was an overall increase in capture of target cells (Fig. S2C), and this increase was unchanged regardless of whether these cells were infected with WT or dU virus (21.5% versus 23.3% or 22%; average of $n = 4$ for mock versus WT and dU, respectively; Fig. 2B). In keeping with an inverse correlation between cell capture efficiency and CD47 expression on target cells, these results

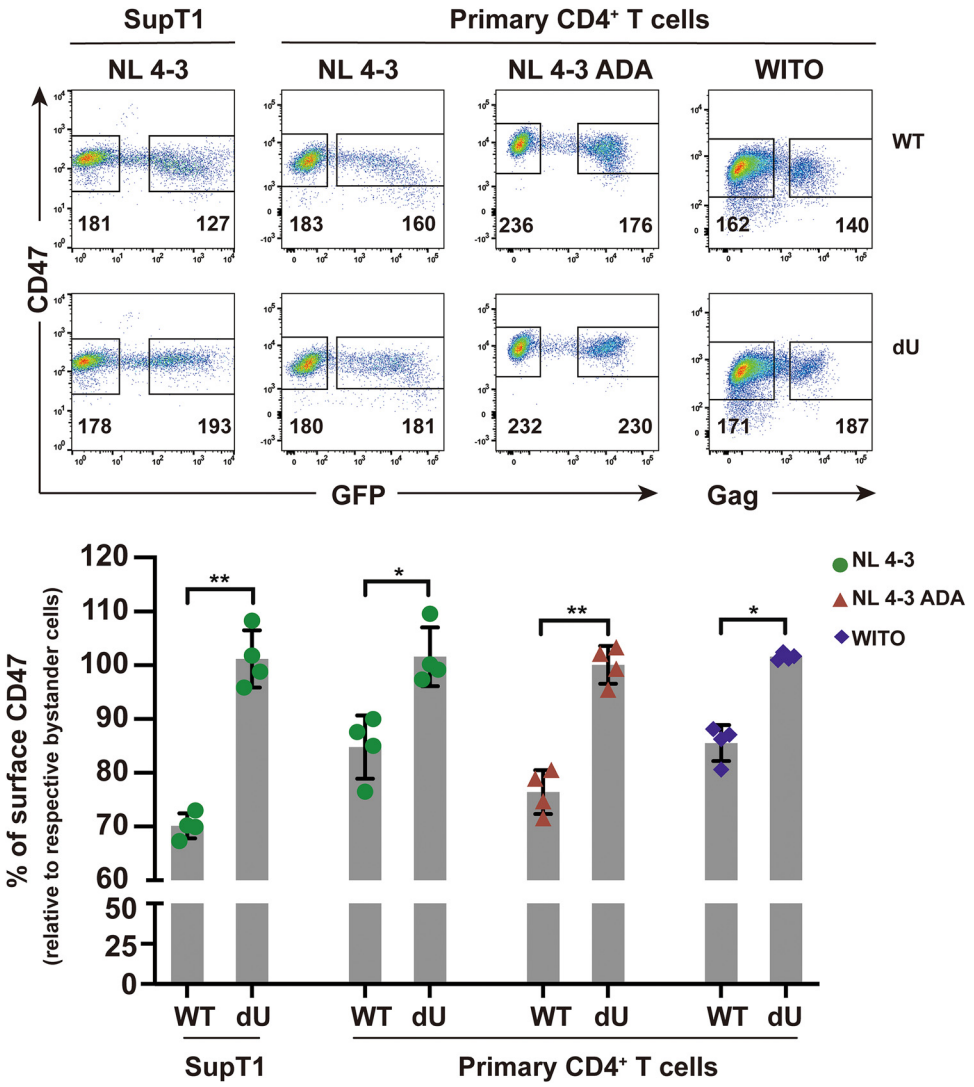

FIG 1 CD47 is downregulated from the surface of HIV-1-infected $CD4^+$ T cells by Vpu. SupT1 T cells or primary $CD4^+$ T cells were infected with GFP-expressing NL4-3 (WT or dU) viruses or with either VSV-G pseudotyped GFP-expressing NL 4-3 ADA (WT or dU) or transmitted/founder WITO (WT or dU) viruses as indicated. After 48 h, cells were stained with anti-CD47 (clone CC2C6) and analyzed by flow cytometry. Top, representative flow cytometry dot plot graphs with indications of the median fluorescence intensity (MFI) values for infected (GFP- or Gag-positive) and bystander cells (GFP- or Gag-negative). Bottom, summary graphs of relative surface CD47 expression levels at 48 h postinfection (hpi) with the indicated viruses ($n = 4$). The percent MFI values were calculated relative to that obtained in the respective bystander cells. Statistical analysis was performed using Mann-Whitney U test (**, $P < 0.01$; *, $P < 0.05$); error bars represent standard deviations (SD). Flow cytometry data for this figure were generated on a CyAn ADP cytometer (Beckman Coulter).

indicate that Vpu-mediated CD47 downregulation enhanced the susceptibility of T cells to be taken up by MDMs.

To directly demonstrate that this process was a consequence of phagocytosis, we performed similar experiments using target cells labeled with pHrodo, a pH-sensitive dye that becomes fluorescent within the acidic environment of phagolysosomes, thus enabling an accurate measurement of bona fide phagocytosis. Indeed, using this approach we also observed a significantly higher frequency of $CD11b^+$/$pHrodo^+$ cells when MDMs were cocultured with WT (6.3%; average of $n = 5$) than when MDMs were cocultured with dU (3.2%; average of $n = 5$) virus-infected targets (Fig. 2C). Also consistent with the data from the capture assay (Fig. 2B; Fig. S2C), CD47KO target cells were more efficiently phagocytosed by MDMs (Fig. S2D), the extent of which was comparable among uninfected, WT virus-infected, or dU virus-infected targets (10.8%, 12.8%,

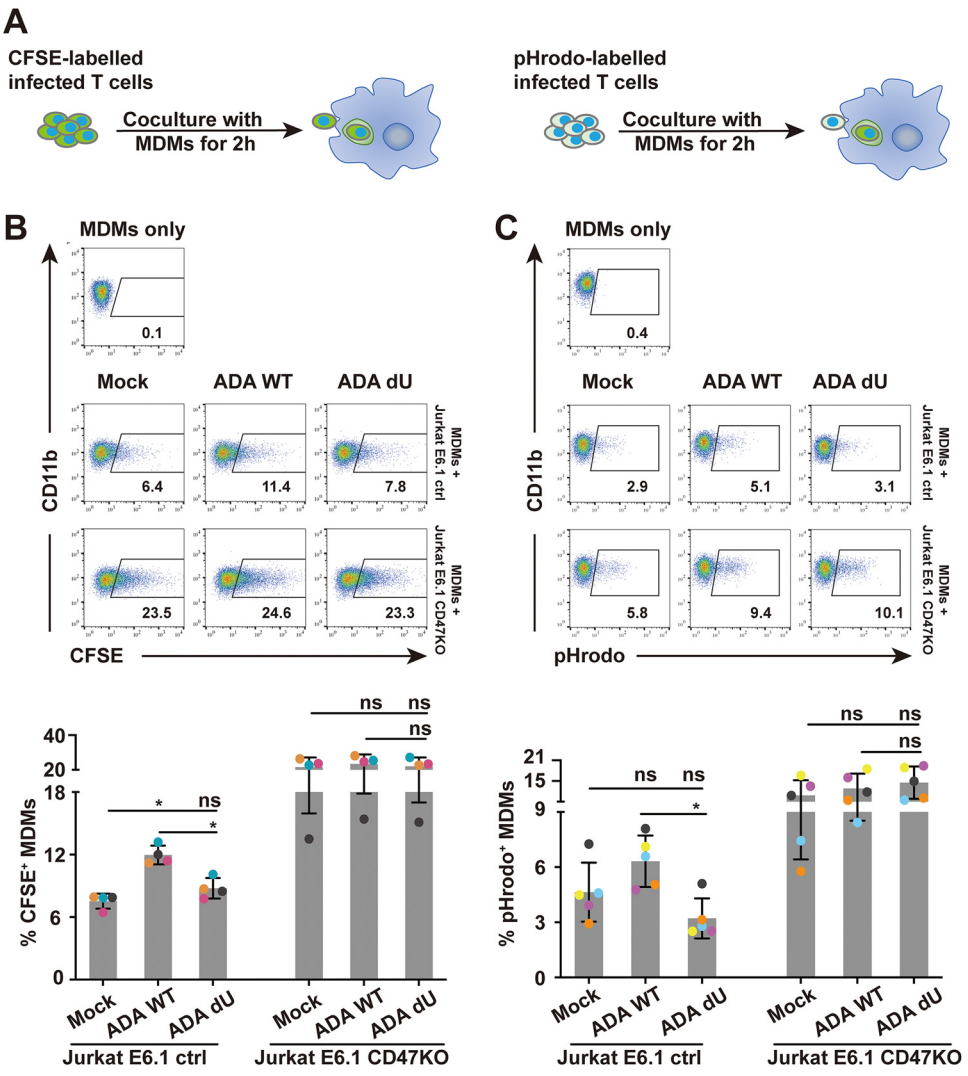

FIG 2 Vpu-mediated CD47 downregulation enhances capture and phagocytosis of infected T cells by MDMs. (A) Experimental strategy for HIV-1-infected target cell labeling and coculture with MDMs for analysis of *in vitro* capture or phagocytosis by flow cytometry. Target cells were either mock infected or infected with VSV-G pseudotyped NL 4-3 ADA (WT or dU) viruses for 48 h and labeled with either CFSE (left) or pHrodo (right). (B) Top, representative flow cytometry dot plots of MDMs ($CD11b^+$) with the percentage of the $CFSE^+$ population corresponding to capture. Bottom, summary graphs for capture of CFSE-labeled CD47-expressing Jurkat E6.1 control (ctrl) or CD47 knockout (KO) Jurkat E6.1 cells by MDMs under the indicated conditions. (C) Top, representative flow cytometry dot plots of MDMs ($CD11b^+$) with percentage of the $pHrodo^+$ population corresponding to phagocytosis. Bottom, summary graphs for phagocytosis of pHrodo-labeled target cells by MDMs under the indicated conditions. Data in panels B and C were analyzed by Mann-Whitney U test (*, $P < 0.05$; ns, nonsignificant, $P > 0.05$); error bars represent SD.

and 14.6%, respectively; average of $n = 5$) (Fig. 2C). Importantly the differential impact of Vpu on the capture and phagocytosis of CD47-expressing T cells was not linked to an increase in the frequency of $Annexin^+$ apoptotic target cells, a condition known to trigger phagocytosis by MDMs (Fig. S2E). Taken together, these results indicate that Vpu promotes both capture and phagocytosis of target cells.

Phagocytosis of infected $CD4^+$ T cells promotes productive infection of MDMs by T/F virus. T/F viruses were reported to display a much weaker tropism for MDMs than truly M-tropic virus strains (27). Indeed, there was no detectable infection (based on intracellular Gag p24) of MDMs using WITO T/F virus (multiplicity of infection (MOI) of 5), whereas infection with a cell-free WT NL 4-3 ADA virus (M-tropic, MOI of 2) resulted in up to 5% of $p24^+$ cells (Fig. S3A). To investigate whether WITO could infect MDMs via phagocytosis of infected primary $CD4^+$ T cells, MDMs were either cocultured with

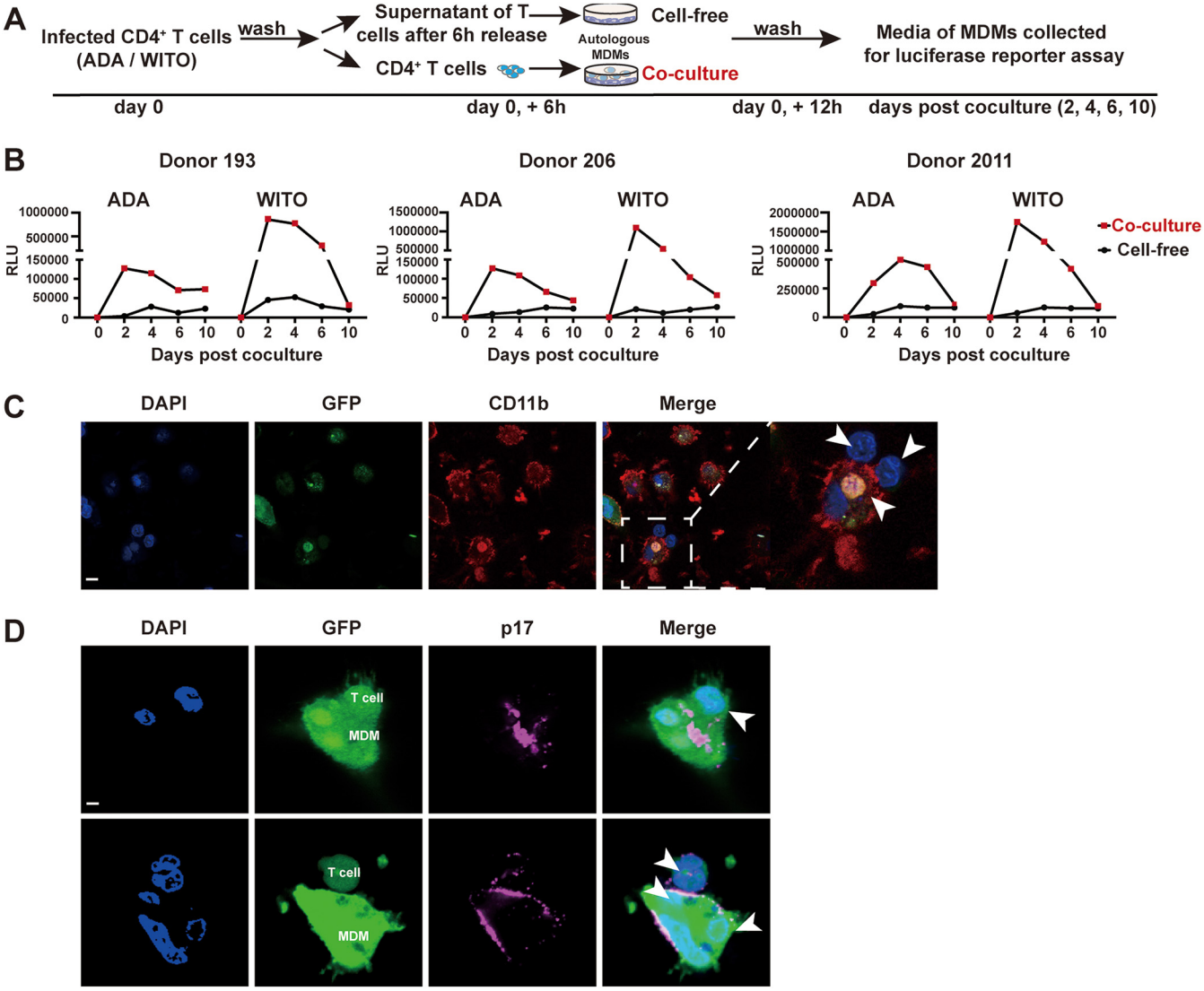

FIG 3 Phagocytosis of infected CD4$^+$ T cells promotes productive infection of MDMs by T/F virus. (A) Experimental strategy for coculture of infected CD4$^+$ T cells with autologous MDMs and analysis of MDM productive infection. MDMs were cocultured for 6 h with WT NL 4-3 ADA- or WITO-infected autologous CD4$^+$ T cells (coculture) or were exposed for 6 h with supernatants from the same HIV-1-infected T cells (cell-free). MDMs were maintained in culture after washing off T cells or supernatants, and medium from MDMs was collected at the indicated time points to assess the production of infectious particles via infection of TZM-bl cells and luciferase (Luc) activity assay. (B) TZM-bl cells were infected for 48 h with medium from MDMs collected at different time points and assayed for Luc activity. Results are expressed as relative light units (RLU). Shown are RLU of TZM-bl cells infected with medium collected from MDMs from 3 donors. (C, D) GFP-expressing NL 4-3 ADA-infected SupT1 cells were cocultured for 2 h with MDMs; cells were then stained with anti-CD11b (C) or anti-p17 Abs (D) as well as DAPI and analyzed by confocal microscopy (scale bar, 10 μm). T cells are indicated by white arrows.

CD4$^+$ T cells infected (to a comparable level; Fig. S3B) with either ADA or WITO viruses or were cultured in the presence of the corresponding virion-containing supernatants from T cell cultures before extensive washes to eliminate input target T cells or virions. The former was referred to as "coculture" while the latter, was designated "cell-free" in Fig. 3. Conditioned supernatant from both "coculture" and "cell-free" infections was collected at various time points and quantified for infectious particles using a TZM-bl cell-based luciferase reporter assay (Fig. 3A). While the medium from cell-free-infected MDMs revealed a modest luciferase activity for both ADA and WITO infections, medium from MDMs cocultured with infected CD4$^+$ T cells showed meaningfully higher levels (Fig. 3B). Interestingly, we observed approximately 6- to 9-fold higher viral production (day 2) for MDMs cocultured with WITO-infected CD4$^+$ T cells than for MDMs cocultured with ADA-infected cells (Fig. 3B), despite the initially comparable infection of CD4$^+$ T cells at the time of the coculture (Fig. S3B). These results show that HIV and

notably T/F viruses can productively infect MDMs through cell-to-cell contact with infected $CD4^+$ T cells. To directly support the notion that capture and engulfment of infected T cells was occurring under these conditions, MDMs cocultured with T cells infected with GFP-marked viruses were processed for immunostaining and analysis by confocal microscopy. As shown in Fig. 3C, the presence of GFP^+ MDMs in close contact with T cells or containing intact GFP^+ T cells could be observed. Furthermore, MDMs displaying a GFP signal following cell contact showed the presence of multiple nuclei and harbored Gag p17 immunostaining in internal compartments as well as at the cell periphery, suggesting the intercellular transfer of fully mature virus particles to MDM (Fig. 3D). Taken together with the capture/phagocytosis data (Fig. 2), we assert that the improved infection of MDMs is likely a consequence of their engulfment of infected $CD4^+$ T cells.

To provide evidence that the infection of MDMs was indeed due to phagocytosis, we introduced jasplakinolide (Jasp) to the cocultures (Fig. 4A). Jasp was reported to promote actin polymerization and stabilize actin filaments, thereby inhibiting cellular processes dependent on actin dynamics, including phagocytosis (28, 36). In brief, MDMs were pretreated with Jasp, cocultured with WITO-infected $CD4^+$ T cells, and analyzed by flow cytometry for phagocytosis activity (Fig. 4B) and the frequency of infected MDMs (Fig. 4C). Treatment of MDMs with Jasp effectively inhibited phagocytosis (Fig. 4B) and blocked the infection (Fig. 4C). Consistent with these findings, the level of infectious viral particles, measured via luciferase activity in TZM-bl cells, was negligible in the supernatant of MDM cultures following Jasp treatment (Fig. 4D). As well, the fact that reverse transcriptase inhibitor zidovudine (AZT) or integrase inhibitor raltegravir (Ral) (Fig. S4A and B) could block MDM infection following coculture of WITO-infected $CD4^+$ T cells further validates the authenticity of the MDM infection.

Given that the effect of actin filament disruption on HIV-1 viral release remained unclear (37), we assessed whether Jasp treatment would affect virion release, which would ultimately interfere with MDM infection. To this end, WITO-infected T cells were washed to remove cell-free virions and then cultured in the presence or absence of Jasp. As shown in Fig. 4E, Jasp treatment did not affect the release of viral particles from T cells. Altogether, using different cell-based assays, we provide evidence that the ability of MDMs to phagocytose infected T cells rendered them susceptible to infection by viruses that would otherwise be poorly infectious.

Vpu facilitates productive infection of macrophages by enhancing phagocytosis of infected T cells through CD47 downregulation. To directly address whether the enhanced uptake of infected T cells that display CD47 downregulation by Vpu results in enhanced infection of macrophages, similar experiments were conducted using WT or dU WITO-infected Jurkat cells as target (Fig. 5A). Consistent with our previous results, we observed a significantly higher frequency of $CD11b^+$/$pHrodo^+$ cells upon coculture of MDMs with WT WITO-infected Jurkat cells (7%; average of $n = 4$) than that observed in cocultures with mock- or dU WITO-infected Jurkat cells (3.2% or 4.6%, respectively; average of $n = 4$; Fig. 5B), a condition that was directly linked to a Vpu-dependent downregulation of CD47 expression at the surface of infected T cells (Fig. S5A) yet was independent from apoptosis (Fig. S5B). Importantly, we found that macrophage infection was generally more efficient upon coculture with T cells infected with WT WITO than upon coculture with T cells infected with Vpu-deficient WITO (Fig. 5C), thus supporting the notion that enhanced phagocytosis of infected T cells by MDMs following Vpu-mediated CD47 downregulation promotes a heightened productive infection of MDMs.

Vpu binds CD47 via its transmembrane domain and targets CD47 for lysosomal degradation. We next sought to understand the mechanism involved in Vpu-mediated CD47 antagonism. HEK 293T cells were cotransfected with plasmids expressing CD47 and Vpu and analyzed by Western blotting for CD47 expression. CD47 was downregulated by Vpu in a dose-dependent manner by as much as 60% (Fig. 6A), raising the question as to how, mechanistically, Vpu mediates the depletion. Thus, we generated Vpu variants that contain mutations within the main functional domains, including (i) A15L-W23A in the TMD that is involved in various target interactions (38, 39), (ii)

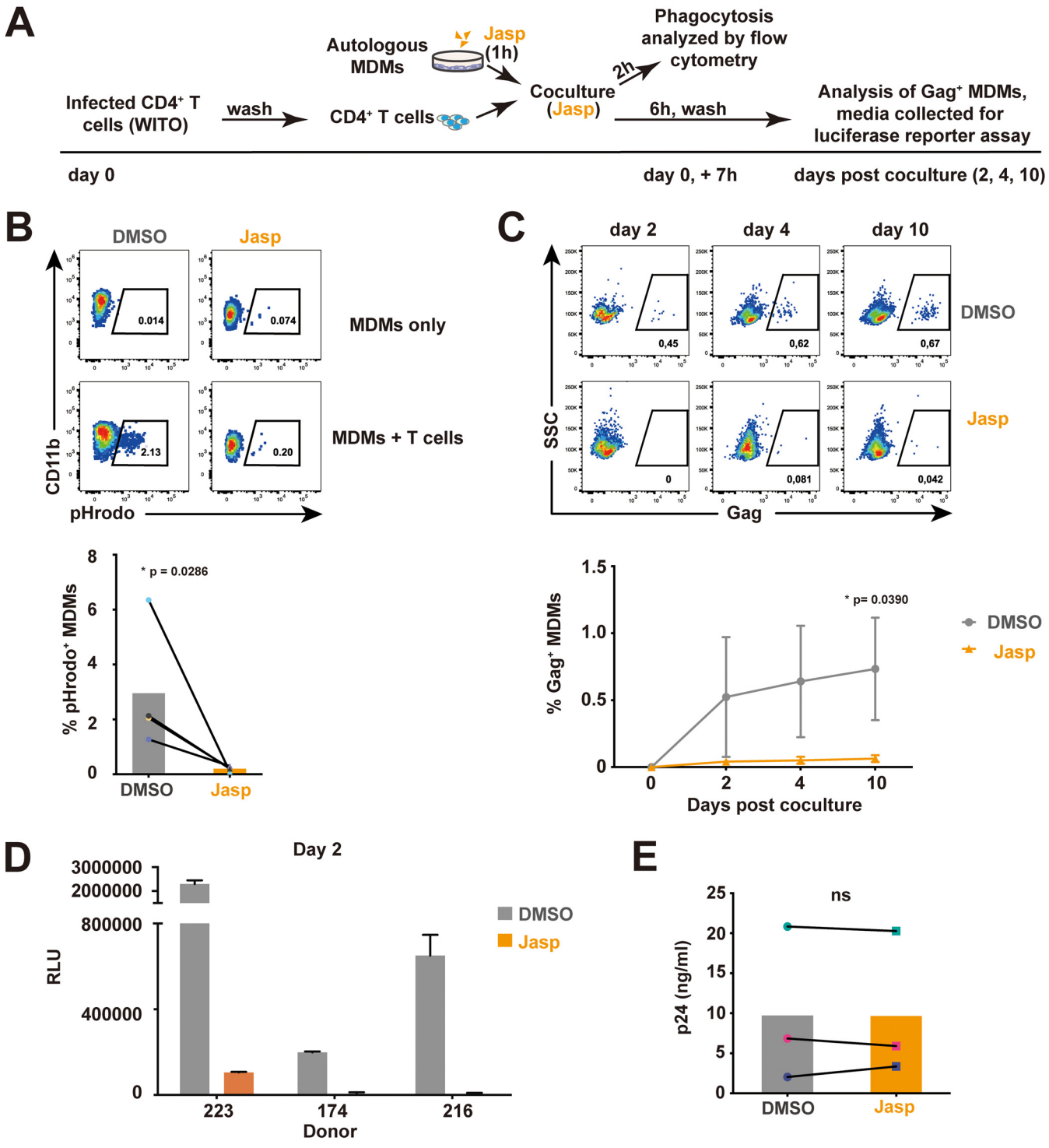

FIG 4 Inhibition of phagocytosis hinders productive infection of MDMs by T/F virus. (A) Experimental strategy for coculture of infected CD4$^+$ T cells, with autologous MDMs pretreated with jasplakinolide (Jasp), and analysis of phagocytosis and MDM productive infection. Pretreated MDMs (1 h with Jasp or vehicle [DMSO]) were cocultured for 6 h with WITO-infected CD4$^+$ T cells in the presence of Jasp or DMSO. MDMs were also cocultured for 2 h with the same number of pHrodo-treated CD4$^+$ T cells and analyzed for phagocytosis by flow cytometry. MDMs were maintained in culture after washing off T cells and were collected at the indicated time points for intracellular Gag staining and flow cytometry analysis. Evaluation of infectious virus production was determined as described above using the TZM-bl assay. (B) Inhibition of phagocytosis by Jasp. Representative flow cytometry dot plots of MDMs (CD11b$^+$) with percentage of pHrodo$^+$ populations corresponding to phagocytosis of CD4$^+$ T cells by MDMs (top) and summary graph (bottom); data were analyzed by Mann-Whitney U test (*, $P < 0.05$). (C) Inhibition of MDM infection by Jasp. Representative flow cytometry dot plots of MDMs showing the percentage of Gag$^+$ cells at the indicated time points (top) following exposure to infected target cells. The summary graph represents the data obtained with MDMs from 3 distinct donors (bottom). (D) TZM-bl cells infected with medium from MDMs cocultured with infected CD4$^+$ T cells were assayed for Luc activity; shown are RLU values detected with medium collected from MDMs from 3 distinct donors. (E) Jasp does not affect viral release from infected CD4$^+$ T cells. WT

(Continued on next page)

the S53/57A mutation within the DSGNES diserine motif that is involved in the recruitment of the Skp1-cullin 1-F-box (SCF)$^{\beta TrCP}$ E3 ubiquitin ligase, responsible for ubiquitination and degradation of several Vpu targets (40, 41), and (iii) $A_{63}XXXA_{67}V$ (AXXXAV for short) within the EXXXLV trafficking motif, which targets Vpu-containing complexes to intracellular compartments away from the plasma membrane (42). To this end, we found that all three Vpu mutants prevented CD47 depletion (Fig. 6B and C; input), suggesting the importance of the main functional domains of Vpu in this process. Indeed, the A15L-W23A mutant was unable to bind CD47 (Fig. 6C), implying that the Vpu TMD mediates complex formation with CD47. To determine whether Vpu induces CD47 protein degradation by either the proteasomal or lysosomal pathway, we treated Vpu- and CD47-expressing HEK 293T transfectants with proteasomal inhibitor MG132 or lysosomal inhibitor concanamycin A (ConA) and found that ConA, but not MG132, prevented CD47 depletion (Fig. 6D). Collectively, these results indicate that Vpu binds CD47 via its TMD and targets the host protein for lysosomal degradation. Conceivably, this process requires both the SCF$^{\beta TrCP}$-recruiting DSGNES diserine motif as well as the EXXXLV trafficking signal, consistent with the lack of CD47 degradation by the S53/57A and AXXXAV mutants.

Furthermore, given that Vpu is typically involved in TMD-TMD interactions with its target proteins, we generated a chimeric CD47 mutant, composed of the extracellular domain (ECD1; amino acids 1 to 141) of human CD47 as well as the five membrane-spanning domains (MSDs) and the cytoplasmic tail (CT) of mouse CD47 (Fig. S6), which displays ~26% of amino acid sequence divergence mainly found in the first and second MSDs. In this configuration, CD47 became largely resistant to Vpu-mediated degradation, consistent with the fact that the mouse CD47 counterpart was insensitive to Vpu (Fig. S6). These results suggest that the MSDs are important determinants of human CD47 susceptibility to Vpu-mediated degradation.

HIV-1-infected cells expressing Vpu-resistant chimeric CD47 are less prone to infect macrophages through phagocytosis. Given that chimeric CD47 was resistant to Vpu-mediated degradation, we next asked if expression of this mutant would alter target cell susceptibility to phagocytosis by MDMs. To this end, we used a CD47KO Jurkat cell line (JC47) (43) to generate cell lines stably expressing either the human-mouse chimeric CD47 (JC47-cCD47) or human CD47 (JC47-hCD47). Cells were selected and enriched by fluorescence-activated cell sorting (FACS) to obtain CD47 expression levels comparable to those detected on the parental Jurkat cells (Fig. 7A). Upon infection of these cell lines with NL 4-3 ADA WT HIV-1, we observed downregulation of CD47 by 40% on JC47-hCD47 cells, but we observed a downregulation of only 10% on those expressing the chimeric JC47-cCD47 (Fig. 7B). Next, we investigated the susceptibility of uninfected (mock) and infected JC47-derived cell lines to phagocytosis by MDMs. First, we found that JC47-hCD47 cells were phagocytosed by MDMs to a similar degree as JC47-cCD47 cells, since both showed ~5% CD11b$^+$/pHrodo$^+$ cells, suggesting that cCD47 was as effective as hCD47 at inducing a "don't-eat-me" signal (Fig. S7A and Fig. 7C). Interestingly, upon infection with WT HIV-1, JC47-hCD47 cells were phagocytosed more efficiently than infected JC47-cCD47 cells (Fig. 7C). Importantly, this difference in phagocytosis was not linked to apoptosis of target cells (Fig. S7B). Furthermore, and in agreement with the phagocytosis results, we observed heightened virus production as measured by luciferase activity from MDMs cocultured with WT HIV-infected JC47-hCD47 cells (Fig. 7D) compared to their chimeric JC47-cCD47 counterparts. Collectively, these results further underscore our observation that Vpu-mediated CD47 downregulation potentiates phagocytosis of infected T cells by MDMs and, consequently, promotes increased productive infection of MDMs.

FIG 4 Legend (Continued)
WITO virus-infected cells were washed to remove cell-associated virions and then treated with Jasp or vehicle DMSO for 6 h. Virus-containing supernatants were collected and quantified for p24 by ELISA. The data shown are the results obtained with CD4$^+$ T cells from 3 distinct donors. Data in panels C and E were analyzed by two-tailed Student's *t* test (*, $P < 0.05$; ns, nonsignificant, $P > 0.05$); error bars represent SD.

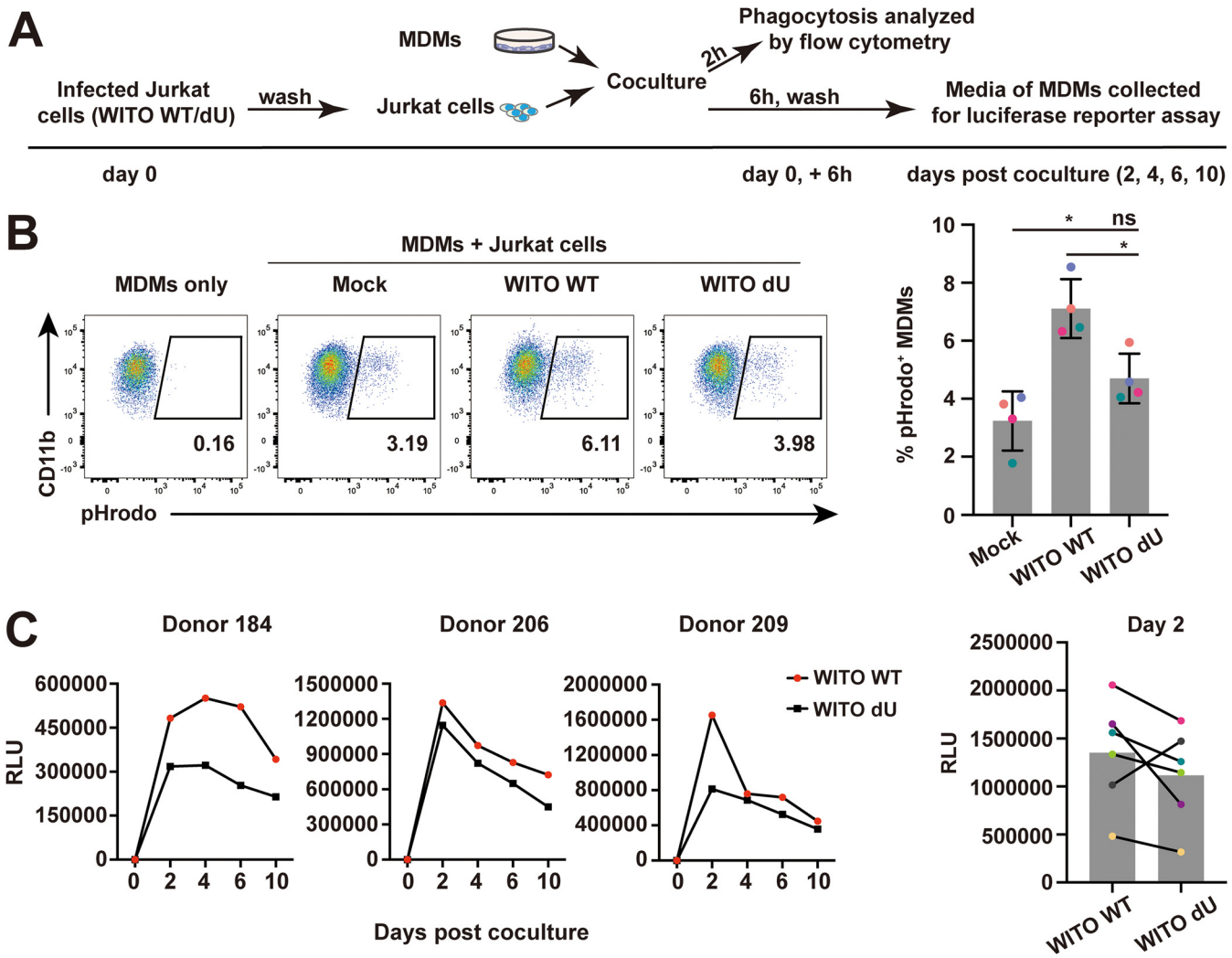

FIG 5 Effect of Vpu on infection of MDMs through phagocytosis of infected Jurkat cells. (A) Experimental strategy for coculture of infected Jurkat E6.1 cells with MDMs and analysis of phagocytosis and MDM productive infection. MDMs were cocultured for 6 h with VSV-G pseudotyped WITO (WT or dU)-infected Jurkat cells. MDMs were also cocultured for 2 h with the same number of pHrodo-treated Jurkat cells and analyzed for phagocytosis by flow cytometry. MDMs were maintained in culture after washing off T cells, and the MDM medium was then collected at the indicated time points for evaluation of infectious virus production using the TZM-bl assay as described above. (B) WITO-infected Jurkat cells are prone to phagocytosis by MDMs in a Vpu-dependent manner. Representative flow cytometry dot plots of MDMs ($CD11b^+$) with percentage of $pHrodo^+$ populations corresponding to phagocytosis (left). Summary graphs for phagocytosis of pHrodo-labeled Jurkat cells by MDMs under the indicated conditions are shown on the right. Data were analyzed by Mann-Whitney U test (*, $P < 0.05$; ns, nonsignificant, $P > 0.05$); error bars represent SD. (C) TZM-bl cells were infected for 48 h with MDM medium collected at different time points and assayed for Luc activity. Shown are RLU values of TZM-bl cells infected with medium collected from MDMs of 3 donors (left); Luc activity of TZM-bl-infected cells with medium collected at day 2 after coculture from distinct donors ($n = 6$, right).

DISCUSSION

In this study, we extend our previous SILAC-based observation that CD47 is a putative target of HIV-1 Vpu (6, 10) and reveal that Vpu indeed downregulates CD47 on $CD4^+$ T cells infected with lab-adapted X4-tropic NL 4-3, R5-tropic NL 4-3 ADA, as well as T/F WITO virus (Fig. 1). These findings obtained in the context of HIV-1 infection are in contrast to those reported by the Hasenkrug group, which showed that CD47 was upregulated in different types of immune cells upon recognition of several pathogens, including severe acute respiratory syndrome coronavirus 2 (SARS-CoV-2), hepatitis C virus (HCV), and lymphocytic choriomeningitis virus (LCMV) (44, 45), suggesting that downregulation of CD47 is an evolved viral countermeasure that provides HIV with a selective advantage. Indeed, we show that Vpu-mediated CD47 downregulation leads to an enhanced capture and phagocytosis of infected $CD4^+$ T cells by MDMs (Fig. 2), a process that ultimately facilitates productive infection of macrophages (Fig. 5). As well,

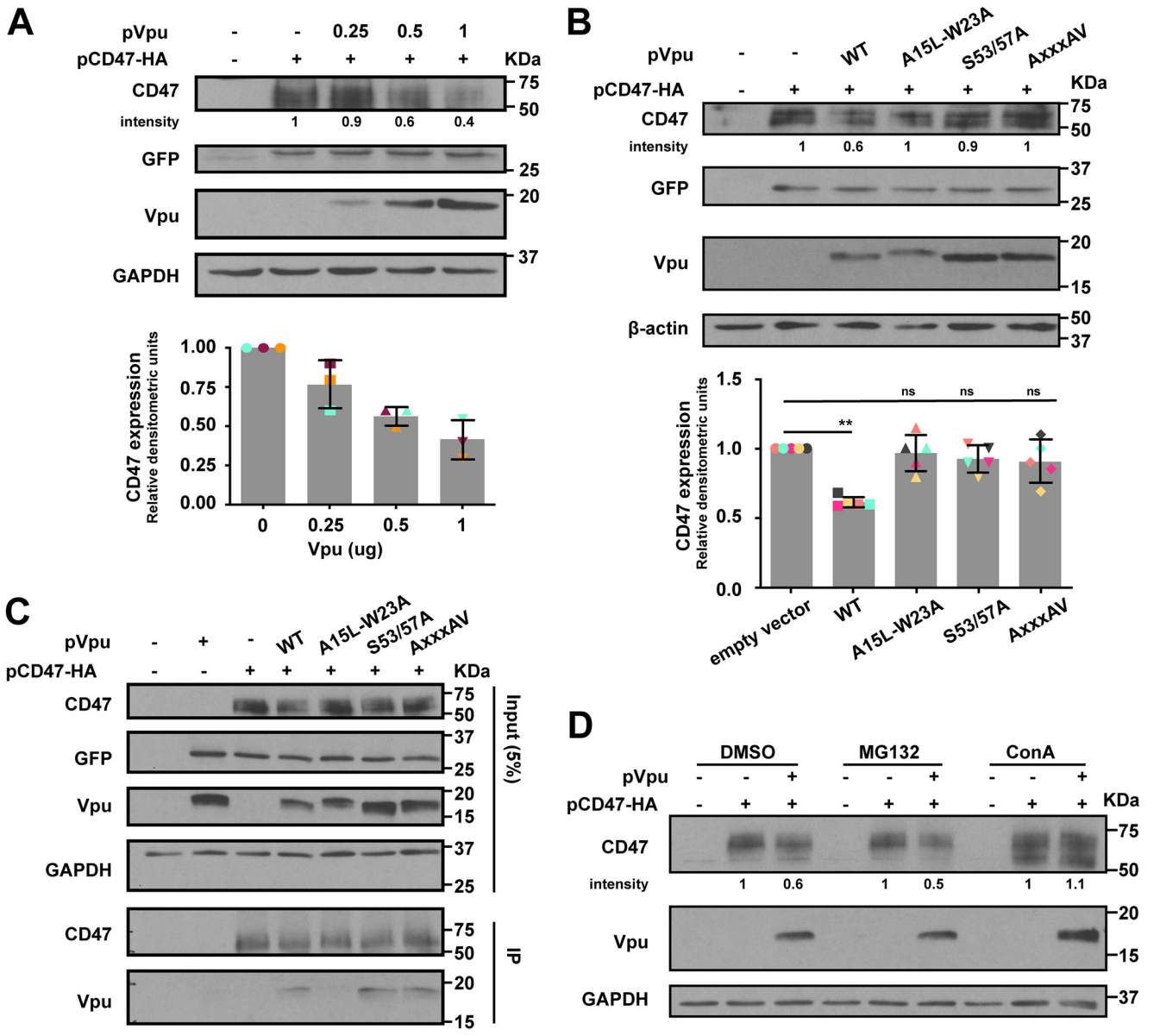

FIG 6 Vpu binds CD47 via its transmembrane domain (TMD) and targets CD47 for lysosomal degradation. (A) Vpu induces depletion of CD47. HEK 293T cells were cotransfected with plasmids encoding HA-tagged CD47 (pCD47-HA) along with increasing concentrations of GFP-marked plasmids expressing wild-type ADA Vpu (pVpu). An empty vector expressing GFP alone was added to adjust the total amounts of plasmid DNA under all conditions. Whole-cell lysates were analyzed for the indicated proteins by Western blotting. A representative blot is shown (top), and a summary graph of densitometric analysis of CD47 is presented (bottom); error bars represent SD. (B) Vpu-mediated CD47 depletion requires the main Vpu functional motifs. HEK 293T were cotransfected with pCD47-HA, along with either empty vector, or plasmids encoding WT Vpu or the indicated Vpu mutants. A representative Western blot is shown (top) as well as a summary graph of densitometric analysis of CD47 (bottom); statistical significance was determined by Mann-Whitney U test (**, $P < 0.01$; ns, nonsignificant, $P > 0.05$); error bars represent SD. (C) HEK 293T cells were cotransfected with the indicated plasmids for 48 h prior to cell lysis and immunoprecipitation (IP) using anti-HA antibody. The immunoprecipitates were analyzed for the indicated proteins by Western blotting. (D) HEK 293T cells were cotransfected with the indicated plasmids for 36 h, and vehicle (DMSO), MG132, or concanamycin A (ConA) were added 8 h before cells were harvested and analyzed by Western blotting.

our data in the context of primary CD4$^+$ T cells show that the R5-tropic WITO T/F virus relies on phagocytosis to efficiently infect MDMs, raising the possibility that phagocytosis of infected cells is an important mechanism through which myeloid cells get productively infected by HIV-1 and is likely consequential for interhost HIV-1 transmission.

Macrophages were reported to engulf HIV-1-infected CD4$^+$ T cells, a process that leads to their own infection (28, 29), but the capture recognition signals remained unclear. Binding of CD47 to SIRPα suppresses multiple prophagocytosis signaling pathways, including those mediated by IgG/FcγR, complement/complement receptors, and

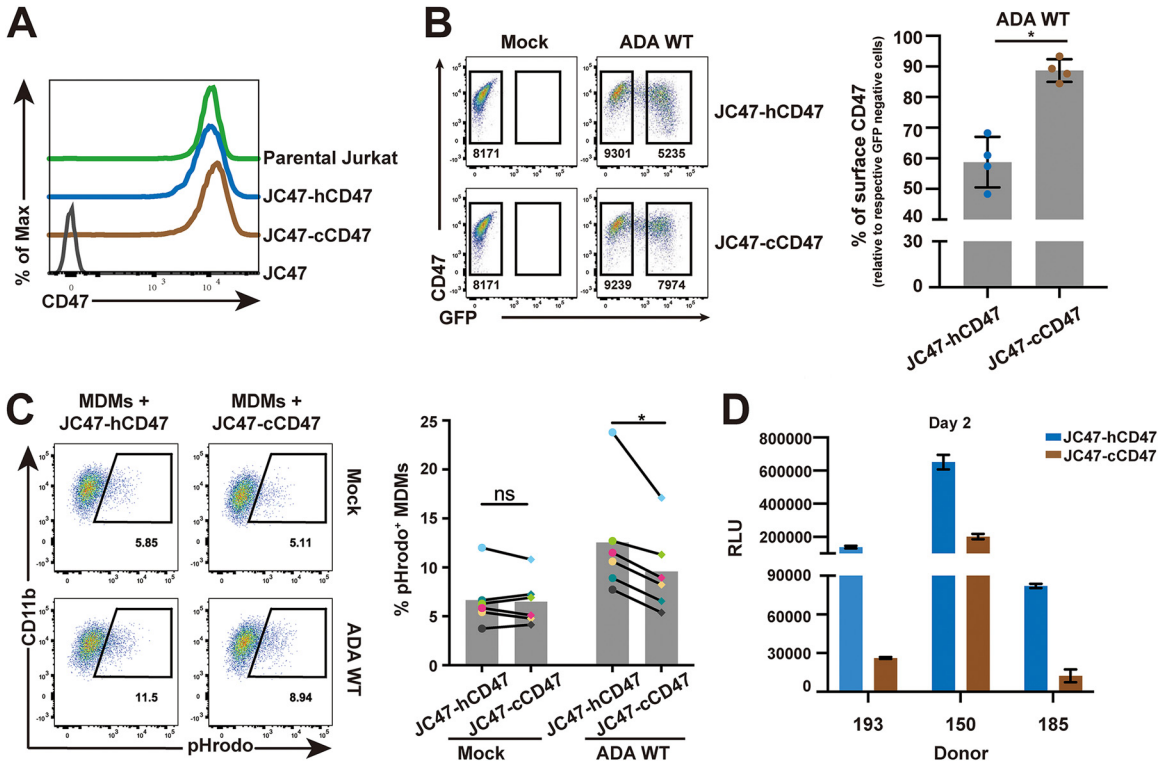

FIG 7 HIV-1-infected CD4$^+$ T cells expressing Vpu-resistant chimeric CD47 are less prone to infect macrophages through phagocytosis. (A) Flow cytometry histogram to validate CD47 surface expression levels in different target Jurkat cell lines, including JC47 (CD47 knockout), JC47-hCD47 (human CD47 reintroduced in JC47), and JC47-cCD47 (chimeric CD47 reintroduced in JC47). (B) JC47-hCD47 and JC47-cCD47 cells were mock infected or infected with VSV-G pseudotyped GFP-expressing WT NL 4-3 ADA virus for 48 h, stained with anti-CD47mAb (clone CC2C6), and analyzed by flow cytometry. Representative flow cytometry dot plot graphs with the MFI values in infected (GFP-positive) and bystander cells (GFP-negative) are shown (left). A summary graph of relative surface CD47 expression levels at 48 h after infection ($n = 4$) is depicted on the right. The percent MFI values were calculated relative to the respective GFP-negative cells. Statistical analysis was performed using Mann-Whitney U test (*, $P < 0.05$); error bars represent SD. (C) The indicated mock- or HIV-1-infected target cells were labeled with pHrodo and cocultured with MDMs for 2 h prior to analysis of MDMs by flow cytometry. Representative flow cytometry dot plots of MDMs (CD11b$^+$) with percentage of pHrodo$^+$ populations corresponding to phagocytosis of target cells by MDMs (left) and a summary graph for MDMs from 6 distinct donors (right) are shown. Data were analyzed by Wilcoxon matched pairs signed rank test (*, $P < 0.05$; ns, nonsignificant, $P > 0.05$). (D) JC47-hCD47 or JC47-cCD47 cells were infected as described and cocultured with MDMs for 6 h. Following removal of infected T cells by washing, MDMs were cultured for 2 days, and MDM medium was collected to infect TZM-bl cells for a luciferase assay. Shown are RLU values detected in media collected from MDMs of 3 distinct donors; error bars represent SD.

calreticulin (46, 47), suggesting that decreased CD47 expression might trigger phagocytosis. Indeed, we show that Vpu-mediated CD47 downregulation enhanced capture and engulfment of infected T cells by MDMs (Fig. 2; Fig. 5B). Although modest, the effect was invariably reproducible and consistent with other studies that used Jurkat cell lines expressing differential surface levels of CD47 as target cells in phagocytosis assays (43, 48). Apart from calreticulin, phosphatidylserine (PS) is another critical pro-phagocytosis signal predominant on apoptotic cells (49). Nevertheless, CD47/SIRPα signaling was recently reported to block the "eat-me" signal driven by PS (50). In the context of HIV-1 infection, we found more externalization of PS on the cell surface as measured by Annexin V staining (Fig. S2E and Fig. S5B in the supplemental material), in line with previously reported results (51). However, although Vpu expression was reported to induce apoptosis (52), we did not observe a significant difference of PS exposure between cells infected with WT and dU HIV-1 (Fig. S2E; Fig. S5B), suggesting that the augmented phagocytosis of cells infected by WT virus was likely resulting from a Vpu-induced decrease of CD47. Indeed, this notion was further supported by our finding that target T cells expressing a human-mouse chimeric form of CD47 that are less responsive to Vpu-mediated downregulation were less prone to phagocytosis by MDMs than human CD47-expressing target cells (Fig. 7C). Furthermore, since we

show that knockout of CD47 in Jurkat T cells results in a strong enhancement of phagocytosis by MDMs (Fig. S2D), our data are collectively consistent with findings showing that lack of CD47 results in augmented phagocytosis of red blood cells (35) and more efficient clearance of lymphohematopoietic cells by macrophages (53). Conversely, target cells with elevated cell surface CD47 are shown to be protected from phagocytosis by macrophages (48, 54).

Infection of macrophages can be detected throughout all stages of HIV-1 infection (26). However, M-tropic viruses are found at late stages of infection and virus isolated at early stages of infection display very limited tropism for macrophages as cell-free virus (17, 25). We hypothesized that through phagocytosis of T/F virus-infected $CD4^+$ T cells, macrophages could become infected with these viruses, a process that would potentially initiate interhost viral dissemination at early stages of HIV-1 infection. Indeed, we found that T/F virus WITO, which poorly infects MDMs by a cell-free route (Fig. S3A) as reported previously (27, 28, 55), was able to elicit a productive infection in MDMs. Interestingly, we observed that phagocytosis of WITO-infected $CD4^+$ T cells ultimately led to an approximately 6- to 9-fold higher viral production by infected MDMs than engulfment of T cells infected with an M-tropic NL 4-3 ADA (Fig. 3B) despite comparable degrees of CD47 downregulation by these viruses (Fig. 1). This implies a potentially more efficient infection of MDMs following uptake of T cells infected with T/F WITO, since the frequency of infected T cells was comparable at the time of phagocytosis (Fig. S3B). This difference in infection efficiency between T/F WITO and HIV ADA may be linked to the differential impact of host antiviral restriction factors and notably interferon-induced transmembrane proteins (IFTIMs), which accumulate intracellularly during HIV-1 infection of macrophages (56, 57) and are incorporated into virions, thus reducing their infectivity (57). In this context, it was reported previously that as IFITM incorporation increased (57), there was a decrease in the infectivity of virions produced by HIV-1 ADA-infected MDMs. In contrast, T/F viruses were reported to be relatively resistant to IFITM-mediated restriction (58, 59), with WITO displaying the most resistance to IFITM3 and releasing the highest levels of infectious virions among all viral strains tested (59). That being said, given the gradual decrease in the level of infectious particles released by MDMs (Fig. 3B; Fig. 5C), it is possible that other restriction factors present in macrophages, including guanylate binding protein 5 (GBP5) (60) and membrane-associated RING-CH 8 (MARCH8) (61), which inhibit the infectivity of macrophage-derived virions, could play a role in controlling viral dissemination.

Phagocytosis is a process known to be important for the elimination of engulfed pathogens and apoptotic cells (62). However, we show that inhibition of phagocytosis by Jasp is linked to a suppression of productive infection of MDMs (Fig. 4), suggesting that HIV-1 takes advantage of this process to infect macrophages. Indeed, a recent study by the Kieffer group (29) in HIV-1-infected humanized mice provided evidence that bone marrow macrophages phagocytosed infected T cells and produced virus within enclosed intracellular compartments. Using electron tomography (ET), they observed macrophages phagocytosing infected T cells, with mature and immature HIV-1 virions within macrophage phagosomes alongside engulfed cells at various degrees of degradation. Moreover, virions were also observed to assemble and undergo budding and maturation within fully enclosed compartments, which would subsequently fuse with surface-accessible invaginations to release virions into the extracellular space. Since HIV-1 virions are inactivated in acidic environments (63), further investigation is needed to better understand how virions escape phagosomal degradation before a complete destruction of the ingested T cells. In fact, many microorganisms have evolved multiple strategies to prevent phagocytic destruction. For instance, *Mycobacterium tuberculosis* inhibits the acidification process of phagosomes via the exclusion of vesicular proton ATPase, thus hindering the maturation of these compartments (64); it also prevents the fusion of lysosomes with phagosomes (65). Interestingly, we show herein that inhibition of reverse transcription and integration suppresses productive infection of MDMs by WITO (Fig. S4), suggesting that

virions transferred to macrophages via phagocytosis of HIV-1-infected T cells were able to actively replicate in MDMs.

While phagocytosis of infected T cells by macrophages represents one route of infection of macrophages, other modes of cell-to-cell virus transfer have also been described *in vitro*. It was recently reported that contacts between infected T lymphocytes and macrophages could lead to virus spreading to macrophages via a two-step fusion process that involves fusion of infected T cells to macrophages and virus transfer to these newly formed lymphocyte/macrophage fused cells. These newly formed cells were in turn able to fuse to neighboring uninfected macrophages, leading to the formation of long-lived virus-producing multinucleated giant cells (MGCs) (66, 67). Although the formation of MGCs has been reported in the lymphoid organs and central nervous system of HIV-1-infected patients (68–70) and SIV-infected macaques (71), the presence of macrophage-T-cell fusion was not observed by the Kieffer group in humanized mice (29).

Experiments directly comparing WT and dU WITO-infected target T cells support the notion that enhanced phagocytosis of infected T cells by MDMs following Vpu-mediated CD47 downregulation facilitates productive infection of macrophages (Fig. 5 and Fig. S5). Considering the conflicting reports about a potential positive or negative effect of BST2 on cell-to-cell transmission (72–75) and its potential impact on phagocytosis and infection of macrophages, we also used a complementary approach that avoided the comparison between WT and dU HIV-infected target T cells. Taking advantage of a Jurkat cell line expressing human-mouse chimeric CD47, which is relatively unresponsive to Vpu modulation (Fig. S6; Fig. 7A and B), we validated that Vpu-mediated CD47 downregulation contributes to phagocytosis of HIV-1-infected $CD4^+$ T cells by MDMs and facilitates productive infection of MDMs (Fig. 7C and D).

Mechanistically, we provide evidence that the main functional domains of Vpu are involved in the downregulation of CD47 and that Vpu interacts with CD47 via its TMD to target the latter for degradation via a lysosomal pathway (Fig. 6). Although the model of CD47 degradation seems rather similar to how Vpu depletes BST2, it remains unclear whether (i) the DSGNES motif through the recruitment of the $SCF^{\beta TRCP1/2}$ complex promotes CD47 ubiquitination and (ii) interaction of adaptor proteins to the EXXXLV trafficking motif of Vpu in complex with CD47 targets CD47 to cellular compartments away from the plasma membrane. More detailed mechanistic studies are required to fully dissect processes underlying Vpu-mediated downregulation of CD47.

In summary, we report herein that CD47 is a new cellular target downregulated by HIV-1 Vpu. Such a decrease in CD47 expression allows for enhanced phagocytosis of infected T cells by macrophages, which ultimately leads to productive infection of this myeloid cell subset even with HIV strains that would otherwise be weakly M-tropic (i.e., T/F viruses). We posit that this process enables macrophages to be infected, including during early stages of HIV infection when M-tropic strains have not yet emerged. Taken together, our data identify a mechanism whereby T/F virus-infected macrophages could be a source of viral reservoirs and promote viral dissemination to different tissues.

MATERIALS AND METHODS

Antibodies. For flow cytometry, the following antibodies (Abs) were used: R-phycoerythrin (PE)/Cy7-conjugated mouse anti-human CD47 (clone CC2C6) monoclonal Ab (MAb) and allophycocyanin (APC)-conjugated anti-CD11b MAb (clone ICRF44) as well as corresponding isotype controls from BioLegend, APC-conjugated mouse anti-human CD47 MAb (clone B6H12, eBioscience), and phycoerythrin (RD1)-conjugated anti-Gag (clone KC57, Beckman Coulter). For immunoprecipitation and Western blotting, the following Abs were used: polyclonal sheep anti-human CD47 (AF4670) and sheep IgG horseradish peroxidase (HRP)-conjugated Ab (HAF016) from R&D Systems; mouse anti-hemagglutinin (HA) MAb (16B12), anti-GAPDH (FF26A/F9), and anti-CRISPR Cas9 (7A9) from BioLegend; rabbit anti-HA MAb (C29F4) from Cell Signaling Technology; rabbit anti-GFP (SAB4301138) from Sigma-Aldrich; anti-β-actin (C4, sc-47778) from Santa Cruz Biotechnology; goat anti-rabbit IgG H+L (HRP, ab205718) and goat anti-mouse IgG H+L (HRP, ab 205719) from Abcam; and anti-Vpu rabbit polyclonal serum as described previously (76). For confocal microscopy analysis, the following Abs were used: purified anti-CD11b (clone ICRF44;

BioLegend), anti-p17 as previously described (77), and Alexa Fluor 594-coupled donkey anti-mouse IgG H+L (Invitrogen, A-21203).

Plasmids. The X4-tropic proviral construct pBR NL 4-3.IRES.GFP wild-type (WT) and its Vpu-deficient derivative (dU) were kindly provided by Frank Kirchhoff (78, 79). The R5-tropic pNL 4-3 ADA.IRES.GFP WT and dU were generated as described (80). The molecular clone of T/F virus WITO was obtained from the NIH AIDS Reagent Program (number 11919) (55), and the dU version of WITO was generated by overlapping PCR.

The pSVCMV-VSV-G plasmid encoding the vesicular stomatitis virus glycoprotein G (VSV-G) was previously described (32). The lentiviral psPAX2 packaging vector was provided by Didier Trono (Addgene plasmid number 12260). The lentivectors lentiCRISPR v2 (plasmid number 52961) (81) and pWPI-IRES-Puro-Ak (plasmid number 154984) were also obtained through Addgene from Feng Zhang and Sonja Best, respectively.

Vpu mutants were generated using PCR-based QuickChange site-directed mutagenesis as per standard protocols (Agilent). Plasmids encoding WT Vpu and Vpu mutants were generated by insertion of the corresponding Vpu fragments from pNL 4-3 ADA proviral constructs into the pCGCG-IRES-GFP plasmid, a kind gift from Frank Kirchhoff (79). The cDNA of human CD47 and mouse CD47 with an HA-tag at the C terminus were purchased from Sino Biological and Thermo Fisher Scientific, respectively. The HA-tag was then added to human CD47 by PCR. Chimeric CD47 consisting of a human extracellular domain and mouse MSD + HA-tagged cytosolic tail was generated by overlapping PCR (see Table S1 in the supplemental material for oligonucleotide primers). These fragments were then inserted into pECFP-N1 (Clonetech). Fragments without the HA tag were also generated by PCR and inserted into pWPI-IRES-Puro-Ak to create pWPI- hCD47 or pWPI-cCD47 for expression of human or chimeric CD47, respectively. All constructs were confirmed by sequencing.

Cell lines. HEK 293T cells and the HeLa TZM-bl indicator cell line were cultured in Dulbecco's Modified Eagle medium (DMEM; Wisent) containing 100 U/ml penicillin and 100 mg/ml streptomycin (P/S) and 10% fetal bovine serum (FBS) (DMEM-10). Lymphocytic cell lines were maintained in RPMI 1640 medium (Wisent) containing P/S and 10% FBS (RPMI-10). SupT1 (Dharam Ablashi [82]) and TZM-bl (John C. Kappes and Xiaoyun Wu [83]) cells were obtained from the NIH AIDS Reagent Program, whereas Jurkat E6.1 and HEK 293T cells were acquired from ATCC. The Jurkat E6.1-based CD47 knockout (KO) cell line, JC47, was cultured as described previously (43).

CD47 knockout and rescue. To generate a CD47KO Jurkat E6.1 cell line, guide sequence 5′-CACCGGATAGCCTATATCCTCGCTG-3′ targeting CD47 was inserted into the lentiCRISPR v2 vector. Lentiviruses were produced by triple transfection of the generated lentivector with psPAX2 and pSVCMV-VSV-G in HEK 293T cells as described previously (6). Control lentiviruses were also produced using the lentiCRISPR v2 without single guide RNA (sgRNA). Jurkat E6.1 cells were transduced with either the control or sgRNA-expressing lentiviruses and selected with puromycin, and the CD47KO population was enriched by fluorescence-activated cell sorting (FACS).

In order to rescue CD47 expression in CD47 KO cells, the JC47 cell line was used. Lentiviruses were produced by transfecting HEK 293T cells with pWPI-hCD47 or pWPI-cCD47 and psPAX2 and pSVCMV-VSV-G. JC47 cells were transduced with lentiviruses expressing either hCD47 or cCD47, selected by CD47 surface expression, and enriched by FACS to ensure that CD47 expression levels were comparable with parental Jurkat E6.1.

Primary cell cultures. Human blood samples were obtained from healthy adult donors following informed consent in accordance with the Declaration of Helsinki under a research protocol approved by the Research Ethics Review Board of the Institut de Recherches Cliniques de Montréal (IRCM). Peripheral blood mononuclear cells (PBMCs) were purified from buffy coats following Ficoll density gradient separation (GE Healthcare). $CD4^+$ T cells were isolated by negative selection using a $CD4^+$ T cell isolation kit (Miltenyi Biotec) according to the manufacturer's protocol. Purified $CD4^+$ T cells were activated with 5 μg/ml phytohemagglutinin-L (PHA-L; Sigma-Aldrich, 11249738001) and 100 U/ml interleukin-2 (IL-2) (PeproTech, 200-02) for 3 days and cultured in RPMI-10 containing 100 U/ml IL-2 for another 2 days before infection.

PBMCs were seeded for 2 h at 37°C in nontissue culture-treated dishes (Fisherbrand) containing serum-free RPMI medium. After gentle washes, adherent cells (which mostly contain monocytes) were cultured for 7 days in RPMI supplemented with 5% decomplemented autologous human blood plasma and 10 ng/ml macrophage colony-stimulating factor (M-CSF) (R&D Systems, 216-MC) to obtain MDMs. Purity of MDMs was determined by CD11b surface staining and was found to routinely reach greater than 95%.

Virus production and infection. Virus stocks were obtained by transfecting HEK 293T cells with proviral DNA in the presence or absence of pSVCMV-VSV-G using polyethylenimine (PEI; Polyscience, 23966). Briefly, HEK 293T cells were plated at 5×10^6 cells per 15-cm dish for overnight incubation and then transfected with 20 μg of total DNA combined with 60 μg of PEI. Medium was changed at 18 h posttransfection. Virus-containing supernatants were collected at 48 h posttransfection, clarified, and pelleted by ultracentrifugation onto a 20% sucrose-phosphate-buffered saline (PBS) cushion for 2 h at 35,000 rpm at 4°C. Viruses were titrated using the TZM-bl indicator cells as previously described (84).

For infection of T cell lines, cells were infected at a multiplicity of infection (MOI) of 0.5 or 1. Primary $CD4^+$ T cells were infected at an MOI of 1 by spin inoculation as previously described (85). MDMs (seeded at 1×10^5 cells/well in 12-well plates) were infected at an MOI of 2 (for NL 4-3 ADA) or an MOI of 5 (for WITO) in 300 μl of RPMI-10. Viruses were adsorbed for 6 h at 37°C before medium was replaced with 1 ml of RPMI-10.

***In vitro* capture and phagocytosis assays.** For flow cytometry-based capture assays, target cells were labeled with 5 μM carboxyfluorescein succinimidyl ester (CFSE) from a CFSE cell proliferation kit

(Invitrogen, C34554) for 5 min at room temperature, washed three times with PBS containing 5% FBS, and resuspended in RPMI with 5% FBS before cells (4×10^5) were added to MDMs and cocultured at 37°C. After 2 h of coculture, MDMs were extensively washed and analyzed by flow cytometry. Capture efficiency was determined as the percentage of $CD11b^+$ cells containing CFSE-derived green fluorescence. For phagocytosis assays, target cells were labeled with 100 ng/ml pHrodo green STP ester (Invitrogen, P35369), pH 7.8, for 30 min at room temperature, resuspended in serum-free RPMI, and then added to MDMs. After 2 h of coculture at 37°C, MDMs were washed, collected, and analyzed. Phagocytosis efficiency was determined as the percentage of $CD11b^+$ cells containing pHrodo-derived green fluorescence.

Coculture experiments of $CD4^+$ T cells with MDMs. $CD4^+$ T cells were infected, and after 2 days, cells were washed and maintained in culture for virus release during a 6-h incubation. Supernatants were separated from T cells by centrifugation ($300 \times g$, 5 min), and a fraction was added to MDMs for "cell-free" and "coculture" infections, respectively. After the 6-h incubation, MDMs were extensively washed to remove supernatants or T cells and cultured for 10 days. The medium from MDMs was collected at specific time intervals for further analysis.

For the experiments involving jasplakinolide (Jasp; Cayman Chemical, 102396-24-7), MDMs were pretreated with 5 μM inhibitor (or vehicle dimethyl sulfoxide [DMSO]) for 1 h. $CD4^+$ T cells were subsequently cocultured with treated or untreated MDMs for 6 h in the presence or absence of Jasp. MDMs were washed extensively after the coculture and analyzed by flow cytometry for phagocytosis of pHrodo-labeled $CD4^+$ target T cells by MDMs, as described above, or maintained in culture for 10 days for a replication kinetics study. The medium from MDMs was collected at day 2 after coculture for measurement of infectious virus production by TZM-bl luciferase reporter assay (see below). To determine the effect of Jasp on virus production, infected $CD4^+$ T cells were washed and incubated with Jasp or DMSO for 6 h, prior to cell supernatant collection for quantification of virus production by HIV-1 p24 enzyme-linked immunosorbent assay (ELISA) (XpressBio).

To assess the effect of reverse transcriptase inhibitor zidovudine (AZT) or integrase inhibitor raltegravir (Ral) on MDM infection, cells were pretreated with 5 μM AZT, 10 μM Ral, or vehicle control DMSO for 2 h and cocultured with infected $CD4^+$ T cells in the presence of the drugs. After 6 h, MDMs were extensively washed to remove the T cells and drugs and then cultured for another 2 days. Efficiency of MDM infection was determined by flow cytometry analysis of intracellular Gag and production of infectious virus in MDM-free culture supernatant using the TZM-bl assay.

For experiments using Jurkat cells infected with VSV-G pseudotyped WITO (WT or dU) viruses as target, cells were extensively washed to remove cell-associated virions 48 h after infection and subsequently cocultured with MDMs for 6 h. MDMs were washed extensively after the coculture and analyzed for phagocytosis or productive infection as described above.

TZM-bl luciferase reporter assay. TZM-bl cells (2×10^4 cells/well seeded in a 24-well plate the previous day) were inoculated with MDM-free culture supernatant for 6 h at 37°C, washed with PBS, and maintained in DMEM-10. At 48 h postinfection, cells were lysed in cell culture lysis reagent (E153A, Promega) and analyzed for luciferase activity using a commercial kit (E1501, Promega).

Confocal microscopy. SupT1 cells were infected with VSV-G pseudotyped GFP-expressing WT NL 4-3 ADA virus for 48 h and cocultured at a ratio of 4:1 with MDMs plated at 1,000 cells/well in an 8-well chamber slide (ibidi, 80806). After 2 h, MDMs were gently washed with PBS and fixed with 4% paraformaldehyde (PFA) for 30 min. Fixed MDMs were incubated for 2 h at 37°C in 5% milk-PBS containing anti-CD11b, a marker of macrophages. To detect p17, fixed MDMs were permeabilized in 0.2% Triton X-100 for 5 min, blocked in PBS containing 5% milk for 15 min, and incubated for 2 h at 37°C in 5% milk-PBS containing anti-p17 Abs, which recognize the mature matrix protein following Gag precursor processing by the viral protease but not the immature Gag precursor (77). Cells were washed and incubated with Alexa Fluor 594-coupled donkey anti-mouse IgG for 30 min at room temperature. Chamber slides were then washed with PBS, and a solution containing 4′,6-diamidino-2-phylindole (DAPI) (0.1 μg/ml in PBS) was applied for 5 min. The slides were washed again and mounted using fluorescent mounting medium. Data were acquired using a laser scanning confocal microscope LSM-710.

HEK 293T cell transfection. HEK 293T cells were transfected with appropriate plasmids using PEI. When applicable, the corresponding empty vectors were included in each transfection to ensure the same amount of transfected DNA under all conditions. For biochemical analyses involving the use of proteasomal and lysosomal inhibitors, MG132 (10 μM; Sigma-Aldrich, 474787) or concanamycin A (ConA; 50 nM; Tocris Bioscience, 2656), respectively, were added to HEK 293T cells 36 h posttransfection. Cells were harvested for analysis 8 h thereafter.

Western blotting. For SDS-PAGE and Western blotting, cells were lysed in radioimmunoprecipitation assay (RIPA)-deoxycholate (DOC) buffer (10 mM Tris pH 7.2, 140 mM NaCl, 8 mM Na_2HPO_4, 2 mM NaH_2PO_4, 1% Nonidet-P40, 0.5% SDS, 1.2 mM deoxycholate) supplemented with protease inhibitors (cOmplete, Roche). Lysates were then mixed with an equal volume of 2× sample buffer (62.5 mM Tris-HCl pH 6.8, 2% SDS, 25% glycerol, 0.01% bromophenol blue, 5% β-mercaptoethanol) and incubated at 37°C for 30 min, as boiling was reported to cause aggregation of CD47 (86). Proteins from lysates were resolved on 15% SDS-PAGE gels, transferred to nitrocellulose membranes, and reacted with primary antibodies. Endogenous CD47 was detected using a sheep polyclonal Ab, and HA-tagged exogenous CD47 was detected using a rabbit MAb (clone C29F4). Membranes were then incubated with HRP-conjugated secondary Abs, and proteins were visualized by enhanced chemiluminescence (ECL).

Coimmunoprecipitation assay. For coimmunoprecipitation studies of Vpu and CD47, transfected HEK 293T cells were lysed in 3-[(3-cholamidopropyl)-dimethylammonio]-1-propanesulfonate (CHAPS) buffer (50 mM Tris, 5 mM EDTA, 100 mM NaCl, 0.5% CHAPS, pH 7.2) supplemented with protease inhibitors. Lysates were first precleared by incubation with 40 μl of protein A-Sepharose beads CL-4B (Sigma,

GE17-0963-03) for 1 h at 4°C and incubated with mouse MAb anti-HA (clone 16B12) overnight. The following day, 40 μl of beads was added, and samples were incubated for 2 h, washed five times with CHAPS buffer, and analyzed by Western blotting.

Flow cytometry. For analysis of CD47 surface expression on T cells, cells were washed with ice-cold PBS/EDTA (5 mM) and stained at 4°C with anti-human CD47 or mouse IgG isotype control diluted in PBS/FBS (1%) for 30 min. Cells were then washed twice with PBS/FBS (1%) and fixed with 1% PFA. Apoptosis of target cells was evaluated using the Annexin V-PI detection kit (eBioscience, 88-8007-72) as per the manufacturer's protocol. For surface staining of MDMs, cells were washed with ice-cold PBS/EDTA (5 mM), detached with Accutase (Sigma-Aldrich, A6964), blocked in PBS/bovine serum albumin (BSA) (1%)/human IgG (blocking buffer) at 4°C for 20 min, and stained for 30 min with anti-human CD11b before additional washing and fixation with 1% PFA. For intracellular Gag staining, $CD4^+$ T cells or MDMs were fixed and permeabilized using the Cytofix/Cytoperm kit (BD Biosciences), according to manufacturer's instructions, and stained with anti-Gag (KC57) at room temperature for 15 min, washed, and resuspended in PBS/FBS (1%).

Flow cytometry data were collected on a Fortessa flow cytometer (BD Bioscience) unless specified otherwise. Cell sorting was conducted on a FacsAria (BD Bioscience). Analyses were performed using FlowJo software version 10.1 for Mac (BD Biosciences).

SUPPLEMENTAL MATERIAL

Supplemental material is available online only.

FIG S1, TIF file, 1 MB.

FIG S2, TIF file, 1.5 MB.

FIG S3, TIF file, 1 MB.

FIG S4, TIF file, 1 MB.

FIG S5, TIF file, 1.2 MB.

FIG S6, TIF file, 1.9 MB.

FIG S7, TIF file, 1.4 MB.

TABLE S1, PDF file, 0.02 MB.

ACKNOWLEDGMENTS

We thank members of our laboratory, especially Robert Lodge, Mariana G. Bego, and Sabelo Lukhele for helpful discussions and critical review of the manuscript and Frédéric Dallaire and Mélanie Laporte for technical support. We also thank Eric Massicotte and Julie Lord (IRCM Flow Cytometry Core) for assistance with flow cytometry, Dominic Filion (IRCM Microscopy and Imaging Core) for microscopy assistance, Odile Neyret and Myriam Rondeau (IRCM Molecular Biology Core) for their support with DNA sequencing, Martine Gauthier (IRCM clinic) for coordinating access to blood donors, and all volunteers for providing blood samples. The following reagents were obtained through the NIH AIDS Reagent Program: SupT1 from D. Ablashi, TZM-bl from J.C. Kappes and X. Wu, and WITO (11919), zidovudine (3485), and raltegravir (11680) from Merck & Company, Inc. This study was supported by grants from the Canadian Institutes of Health Research (CIHR) (FDN 154324), the CIHR supported Canadian HIV Cure Enterprise 2 (CanCURE 2.0) (HB2 164064), and the Fonds de Recherche du Québec-Santé AIDS and Infectious Disease Network to É.A.C. L.C. was supported by studentships from the IRCM and Université de Montréal. É.A.C. is the recipient of the IRCM-Université de Montréal Chair of Excellence in HIV Research.

REFERENCES

1. Neil SJ, Zang T, Bieniasz PD. 2008. Tetherin inhibits retrovirus release and is antagonized by HIV-1 Vpu. Nature 451:425–430. https://doi.org/10.1038/nature06553.
2. Van Damme N, Goff D, Katsura C, Jorgenson RL, Mitchell R, Johnson MC, Stephens EB, Guatelli J. 2008. The interferon-induced protein BST-2 restricts HIV-1 release and is downregulated from the cell surface by the viral Vpu protein. Cell Host Microbe 3:245–252. https://doi.org/10.1016/j.chom.2008.03.001.
3. Wildum S, Schindler M, Munch J, Kirchhoff F. 2006. Contribution of Vpu, Env, and Nef to CD4 down-modulation and resistance of human immunodeficiency virus type 1-infected T cells to superinfection. J Virol 80:8047–8059. https://doi.org/10.1128/JVI.00252-06.
4. Pham TN, Lukhele S, Hajjar F, Routy JP, Cohen EA. 2014. HIV Nef and Vpu protect HIV-infected $CD4^+$ T cells from antibody-mediated cell lysis through down-modulation of CD4 and BST2. Retrovirology 11:15. https://doi.org/10.1186/1742-4690-11-15.
5. Sugden SM, Bego MG, Pham TN, Cohen EA. 2016. Remodeling of the host cell plasma membrane by HIV-1 Nef and Vpu: a strategy to ensure viral fitness and persistence. Viruses 8:67. https://doi.org/10.3390/v8030067.
6. Sugden SM, Pham TN, Cohen EA. 2017. HIV-1 Vpu downmodulates ICAM-1 expression, resulting in decreased killing of infected $CD4^+$ T cells by NK cells. J Virol 91:e02442-16. https://doi.org/10.1128/JVI.02442-16.
7. Jain P, Boso G, Langer S, Soonthornvacharin S, De Jesus PD, Nguyen Q, Olivieri KC, Portillo AJ, Yoh SM, Pache L, Chanda SK. 2018. Large-scale arrayed analysis of protein degradation reveals cellular targets for HIV-1 Vpu. Cell Rep 22:2493–2503. https://doi.org/10.1016/j.celrep.2018.01.091.
8. Liu Y, Fu Y, Wang Q, Li M, Zhou Z, Dabbagh D, Fu C, Zhang H, Li S, Zhang T, Gong J, Kong X, Zhai W, Su J, Sun J, Zhang Y, Yu XF, Shao Z, Zhou F, Wu Y, Tan X. 2019. Proteomic profiling of HIV-1 infection of human $CD4^+$ T cells identifies PSGL-1 as an HIV restriction factor. Nat Microbiol 4:813–825. https://doi.org/10.1038/s41564-019-0372-2.

9. Prevost J, Edgar CR, Richard J, Trothen SM, Jacob RA, Mumby MJ, Pickering S, Dube M, Kaufmann DE, Kirchhoff F, Neil SJD, Finzi A, Dikeakos JD. 2020. HIV-1 Vpu downregulates Tim-3 from the surface of infected CD4$^+$ T cells. J Virol 94:e01999-19. https://doi.org/10.1128/JVI.01999-19.
10. Matheson NJ, Sumner J, Wals K, Rapiteanu R, Weekes MP, Vigan R, Weinelt J, Schindler M, Antrobus R, Costa AS, Frezza C, Clish CB, Neil SJ, Lehner PJ. 2015. Cell surface proteomic map of HIV infection reveals antagonism of amino acid metabolism by Vpu and Nef. Cell Host Microbe 18:409–423. https://doi.org/10.1016/j.chom.2015.09.003.
11. Brown EJ, Frazier WA. 2001. Integrin-associated protein (CD47) and its ligands. Trends Cell Biol 11:130–135. https://doi.org/10.1016/s0962-8924(00)01906-1.
12. Oldenborg PA. 2013. CD47: a cell surface glycoprotein which regulates multiple functions of hematopoietic cells in health and disease. ISRN Hematol 2013:614619. https://doi.org/10.1155/2013/614619.
13. Barclay AN, Van den Berg TK. 2014. The interaction between signal regulatory protein alpha (SIRPα) and CD47: structure, function, and therapeutic target. Annu Rev Immunol 32:25–50. https://doi.org/10.1146/annurev-immunol-032713-120142.
14. Myers LM, Tal MC, Torrez Dulgeroff LB, Carmody AB, Messer RJ, Gulati G, Yiu YY, Staron MM, Angel CL, Sinha R, Markovic M, Pham EA, Fram B, Ahmed A, Newman AM, Glenn JS, Davis MM, Kaech SM, Weissman IL, Hasenkrug KJ. 2019. A functional subset of CD8$^+$ T cells during chronic exhaustion is defined by SIRPα expression. Nat Commun 10:794. https://doi.org/10.1038/s41467-019-08637-9.
15. Hirayama D, Iida T, Nakase H. 2017. The phagocytic function of macrophage-enforcing innate immunity and tissue homeostasis. Int J Mol Sci 19:92. https://doi.org/10.3390/ijms19010092.
16. Shen R, Richter HE, Clements RH, Novak L, Huff K, Bimczok D, Sankaran-Walters S, Dandekar S, Clapham PR, Smythies LE, Smith PD. 2009. Macrophages in vaginal but not intestinal mucosa are monocyte-like and permissive to human immunodeficiency virus type 1 infection. J Virol 83:3258–3267. https://doi.org/10.1128/JVI.01796-08.
17. Sattentau QJ, Stevenson M. 2016. Macrophages and HIV-1: an unhealthy constellation. Cell Host Microbe 19:304–310. https://doi.org/10.1016/j.chom.2016.02.013.
18. Swingler S, Mann AM, Zhou J, Swingler C, Stevenson M. 2007. Apoptotic killing of HIV-1-infected macrophages is subverted by the viral envelope glycoprotein. PLoS Pathog 3:1281–1290. https://doi.org/10.1371/journal.ppat.0030134.
19. Clayton KL, Collins DR, Lengieza J, Ghebremichael M, Dotiwala F, Lieberman J, Walker BD. 2018. Resistance of HIV-infected macrophages to CD8$^+$ T lymphocyte-mediated killing drives activation of the immune system. Nat Immunol 19:475–486. https://doi.org/10.1038/s41590-018-0085-3.
20. Yukl SA, Sinclair E, Somsouk M, Hunt PW, Epling L, Killian M, Girling V, Li P, Havlir DV, Deeks SG, Wong JK, Hatano H. 2014. A comparison of methods for measuring rectal HIV levels suggests that HIV DNA resides in cells other than CD4$^+$ T cells, including myeloid cells. AIDS 28:439–442. https://doi.org/10.1097/QAD.0000000000000166.
21. Ganor Y, Real F, Sennepin A, Dutertre CA, Prevedel L, Xu L, Tudor D, Charmeteau B, Couedel-Courteille A, Marion S, Zenak AR, Jourdain JP, Zhou Z, Schmitt A, Capron C, Eugenin EA, Cheynier R, Revol M, Cristofari S, Hosmalin A, Bomsel M. 2019. HIV-1 reservoirs in urethral macrophages of patients under suppressive antiretroviral therapy. Nat Microbiol 4:633–644. https://doi.org/10.1038/s41564-018-0335-z.
22. Zalar A, Figueroa MI, Ruibal-Ares B, Bare P, Cahn P, de Bracco MM, Belmonte L. 2010. Macrophage HIV-1 infection in duodenal tissue of patients on long term HAART. Antiviral Res 87:269–271. https://doi.org/10.1016/j.antiviral.2010.05.005.
23. Andrade VM, Mavian C, Babic D, Cordeiro T, Sharkey M, Barrios L, Brander C, Martinez-Picado J, Dalmau J, Llano A, Li JZ, Jacobson J, Lavine CL, Seaman MS, Salemi M, Stevenson M. 2020. A minor population of macrophage-tropic HIV-1 variants is identified in recrudescing viremia following analytic treatment interruption. Proc Natl Acad Sci U S A 117:9981–9990. https://doi.org/10.1073/pnas.1917034117.
24. Shen R, Richter HE, Smith PD. 2011. Early HIV-1 target cells in human vaginal and ectocervical mucosa. Am J Reprod Immunol 65:261–267. https://doi.org/10.1111/j.1600-0897.2010.00939.x.
25. Arrildt KT, LaBranche CC, Joseph SB, Dukhovlinova EN, Graham WD, Ping LH, Schnell G, Sturdevant CB, Kincer LP, Mallewa M, Heyderman RS, Rie AV, Cohen MS, Spudich S, Price RW, Montefiori DC, Swanstrom R. 2015. Phenotypic correlates of HIV-1 macrophage tropism. J Virol 89:11294–11311. https://doi.org/10.1128/JVI.00946-15.
26. Koppensteiner H, Brack-Werner R, Schindler M. 2012. Macrophages and their relevance in human immunodeficiency virus type I infection. Retrovirology 9:82. https://doi.org/10.1186/1742-4690-9-82.
27. Ochsenbauer C, Edmonds TG, Ding H, Keele BF, Decker J, Salazar MG, Salazar-Gonzalez JF, Shattock R, Haynes BF, Shaw GM, Hahn BH, Kappes JC. 2012. Generation of transmitted/founder HIV-1 infectious molecular clones and characterization of their replication capacity in CD4 T lymphocytes and monocyte-derived macrophages. J Virol 86:2715–2728. https://doi.org/10.1128/JVI.06157-11.
28. Baxter AE, Russell RA, Duncan CJ, Moore MD, Willberg CB, Pablos JL, Finzi A, Kaufmann DE, Ochsenbauer C, Kappes JC, Groot F, Sattentau QJ. 2014. Macrophage infection via selective capture of HIV-1-infected CD4$^+$ T cells. Cell Host Microbe 16:711–721. https://doi.org/10.1016/j.chom.2014.10.010.
29. Ladinsky MS, Khamaikawin W, Jung Y, Lin S, Lam J, An DS, Bjorkman PJ, Kieffer C. 2019. Mechanisms of virus dissemination in bone marrow of HIV-1-infected humanized BLT mice. eLife 8:e46916. https://doi.org/10.7554/eLife.46916.
30. Calantone N, Wu F, Klase Z, Deleage C, Perkins M, Matsuda K, Thompson EA, Ortiz AM, Vinton CL, Ourmanov I, Lore K, Douek DC, Estes JD, Hirsch VM, Brenchley JM. 2014. Tissue myeloid cells in SIV-infected primates acquire viral DNA through phagocytosis of infected T cells. Immunity 41:493–502. https://doi.org/10.1016/j.immuni.2014.08.014.
31. Norris PJ, Pappalardo BL, Custer B, Spotts G, Hecht FM, Busch MP. 2006. Elevations in IL-10, TNF-α, and IFN-γ from the earliest point of HIV type 1 infection. AIDS Res Hum Retroviruses 22:757–762. https://doi.org/10.1089/aid.2006.22.757.
32. Bego MG, Cote E, Aschman N, Mercier J, Weissenhorn W, Cohen EA. 2015. Vpu exploits the cross-talk between BST2 and the ILT7 receptor to suppress anti-HIV-1 responses by plasmacytoid dendritic cells. PLoS Pathog 11:e1005024. https://doi.org/10.1371/journal.ppat.1005024.
33. Kupzig S, Korolchuk V, Rollason R, Sugden A, Wilde A, Banting G. 2003. Bst-2/HM1.24 is a raft-associated apical membrane protein with an unusual topology. Traffic 4:694–709. https://doi.org/10.1034/j.1600-0854.2003.00129.x.
34. Logtenberg MEW, Jansen JHM, Raaben M, Toebes M, Franke K, Brandsma AM, Matlung HL, Fauster A, Gomez-Eerland R, Bakker NAM, van der Schot S, Marijt KA, Verdoes M, Haanen J, van den Berg JH, Neefjes J, van den Berg TK, Brummelkamp TR, Leusen JHW, Scheeren FA, Schumacher TN. 2019. Glutaminyl cyclase is an enzymatic modifier of the CD47$^-$ SIRPα axis and a target for cancer immunotherapy. Nat Med 25:612–619. https://doi.org/10.1038/s41591-019-0356-z.
35. Oldenborg PA, Zheleznyak A, Fang YF, Lagenaur CF, Gresham HD, Lindberg FP. 2000. Role of CD47 as a marker of self on red blood cells. Science 288:2051–2054. https://doi.org/10.1126/science.288.5473.2051.
36. Bubb MR, Senderowicz AM, Sausville EA, Duncan KL, Korn ED. 1994. Jasplakinolide, a cytotoxic natural product, induces actin polymerization and competitively inhibits the binding of phalloidin to F-actin. J Biol Chem 269:14869–14871. https://doi.org/10.1016/S0021-9258(17)36545-6.
37. Ospina Stella A, Turville S. 2018. All-round manipulation of the actin cytoskeleton by HIV. Viruses 10:63. https://doi.org/10.3390/v10020063.
38. Vigan R, Neil SJD. 2010. Determinants of tetherin antagonism in the transmembrane domain of the human immunodeficiency virus type 1 Vpu protein. J Virol 84:12958–12970. https://doi.org/10.1128/JVI.01699-10.
39. Magadan JG, Bonifacino JS. 2012. Transmembrane domain determinants of CD4 downregulation by HIV-1 Vpu. J Virol 86:757–772. https://doi.org/10.1128/JVI.05933-11.
40. Kueck T, Foster TL, Weinelt J, Sumner JC, Pickering S, Neil SJD. 2015. Serine phosphorylation of HIV-1 Vpu and its binding to tetherin regulates interaction with clathrin adaptors. PLoS Pathog 11:e1005141. https://doi.org/10.1371/journal.ppat.1005141.
41. Margottin F, Bour SP, Durand H, Selig L, Benichou S, Richard V, Thomas D, Strebel K, Benarous R. 1998. A novel human WD protein, h-βTrCp, that interacts with HIV-1 Vpu connects CD4 to the ER degradation pathway through an F-box motif. Mol Cell 1:565–574. https://doi.org/10.1016/S1097-2765(00)80056-8.
42. Kueck T, Neil SJD. 2012. A cytoplasmic tail determinant in HIV-1 Vpu mediates targeting of tetherin for endosomal degradation and counteracts interferon-induced restriction. PLoS Pathog 8:e1002609. https://doi.org/10.1371/journal.ppat.1002609.
43. Leclair P, Liu CC, Monajemi M, Reid GS, Sly LM, Lim CJ. 2018. CD47-ligation induced cell death in T-acute lymphoblastic leukemia. Cell Death Dis 9:544. https://doi.org/10.1038/s41419-018-0601-2.
44. Cham LB, Torrez Dulgeroff LB, Tal MC, Adomati T, Li F, Bhat H, Huang A, Lang PA, Moreno ME, Rivera JM, Galkina SA, Kosikova G, Stoddart CA, McCune JM, Myers LM, Weissman IL, Lang KS, Hasenkrug KJ. 2020.

Immunotherapeutic blockade of CD47 inhibitory signaling enhances innate and adaptive immune responses to viral infection. Cell Rep 31: 107494. https://doi.org/10.1016/j.celrep.2020.03.058.
45. Tal MC, Torrez Dulgeroff LB, Myers L, Cham LB, Mayer-Barber KD, Bohrer AC, Castro E, Yiu YY, Lopez Angel C, Pham E, Carmody AB, Messer RJ, Gars E, Kortmann J, Markovic M, Hasenkrug M, Peterson KE, Winkler CW, Woods TA, Hansen P, Galloway S, Wagh D, Fram BJ, Nguyen T, Corey D, Kalluru RS, Banaei N, Rajadas J, Monack DM, Ahmed A, Sahoo D, Davis MM, Glenn JS, Adomati T, Lang KS, Weissman IL, Hasenkrug KJ. 2020. Up-regulation of CD47 is a host checkpoint response to pathogen recognition. mBio 11:e01293-20. https://doi.org/10.1128/mBio.01293-20.
46. Oldenborg PA, Gresham HD, Lindberg FP. 2001. CD47-signal regulatory protein α (SIRPα) regulates Fcγ and complement receptor-mediated phagocytosis. J Exp Med 193:855–862. https://doi.org/10.1084/jem.193.7.855.
47. Gardai SJ, McPhillips KA, Frasch SC, Janssen WJ, Starefeldt A, Murphy-Ullrich JE, Bratton DL, Oldenborg PA, Michalak M, Henson PM. 2005. Cell-surface calreticulin initiates clearance of viable or apoptotic cells through *trans*-activation of LRP on the phagocyte. Cell 123:321–334. https://doi.org/10.1016/j.cell.2005.08.032.
48. Berkovits BD, Mayr C. 2015. Alternative 3′ UTRs act as scaffolds to regulate membrane protein localization. Nature 522:363–367. https://doi.org/10.1038/nature14321.
49. Barth ND, Marwick JA, Vendrell M, Rossi AG, Dransfield I. 2017. The "phagocytic synapse" and clearance of apoptotic cells. Front Immunol 8:1708. https://doi.org/10.3389/fimmu.2017.01708.
50. Morrissey MA, Kern N, Vale RD. 2020. CD47 ligation repositions the inhibitory receptor SIRPA to suppress integrin activation and phagocytosis. Immunity 53:290–302. https://doi.org/10.1016/j.immuni.2020.07.008.
51. Zaitseva E, Zaitsev E, Melikov K, Arakelyan A, Marin M, Villasmil R, Margolis LB, Melikyan GB, Chernomordik LV. 2017. Fusion stage of HIV-1 entry depends on virus-induced cell surface exposure of phosphatidylserine. Cell Host Microbe 22:99–110. https://doi.org/10.1016/j.chom.2017.06.012.
52. Akari H, Bour S, Kao S, Adachi A, Strebel K. 2001. The human immunodeficiency virus type 1 accessory protein Vpu induces apoptosis by suppressing the nuclear factor κB-dependent expression of antiapoptotic factors. J Exp Med 194:1299–1311. https://doi.org/10.1084/jem.194.9.1299.
53. Blazar BR, Lindberg FP, Ingulli E, Panoskaltsis-Mortari A, Oldenborg PA, Iizuka K, Yokoyama WM, Taylor PA. 2001. CD47 (integrin-associated protein) engagement of dendritic cell and macrophage counterreceptors is required to prevent the clearance of donor lymphohematopoietic cells. J Exp Med 194:541–549. https://doi.org/10.1084/jem.194.4.541.
54. Jaiswal S, Jamieson CH, Pang WW, Park CY, Chao MP, Majeti R, Traver D, van Rooijen N, Weissman IL. 2009. CD47 is upregulated on circulating hematopoietic stem cells and leukemia cells to avoid phagocytosis. Cell 138: 271–285. https://doi.org/10.1016/j.cell.2009.05.046.
55. Salazar-Gonzalez JF, Salazar MG, Keele BF, Learn GH, Giorgi EE, Li H, Decker JM, Wang S, Baalwa J, Kraus MH, Parrish NF, Shaw KS, Guffey MB, Bar KJ, Davis KL, Ochsenbauer-Jambor C, Kappes JC, Saag MS, Cohen MS, Mulenga J, Derdeyn CA, Allen S, Hunter E, Markowitz M, Hraber P, Perelson AS, Bhattacharya T, Haynes BF, Korber BT, Hahn BH, Shaw GM. 2009. Genetic identity, biological phenotype, and evolutionary pathways of transmitted/founder viruses in acute and early HIV-1 infection. J Exp Med 206:1273–1289. https://doi.org/10.1084/jem.20090378.
56. Woelk CH, Ottones F, Plotkin CR, Du P, Royer CD, Rought SE, Lozach J, Sasik R, Kornbluth RS, Richman DD, Corbeil J. 2004. Interferon gene expression following HIV type 1 infection of monocyte-derived macrophages. AIDS Res Hum Retroviruses 20:1210–1222. https://doi.org/10.1089/aid.2004.20.1210.
57. Tartour K, Appourchaux R, Gaillard J, Nguyen XN, Durand S, Turpin J, Beaumont E, Roch E, Berger G, Mahieux R, Brand D, Roingeard P, Cimarelli A. 2014. IFITM proteins are incorporated onto HIV-1 virion particles and negatively imprint their infectivity. Retrovirology 11:103. https://doi.org/10.1186/s12977-014-0103-y.
58. Foster TL, Wilson H, Iyer SS, Coss K, Doores K, Smith S, Kellam P, Finzi A, Borrow P, Hahn BH, Neil SJD. 2016. Resistance of transmitted founder HIV-1 to IFITM-mediated restriction. Cell Host Microbe 20:429–442. https://doi.org/10.1016/j.chom.2016.08.006.
59. Wang Y, Pan Q, Ding S, Wang Z, Yu J, Finzi A, Liu SL, Liang C. 2017. The V3 loop of HIV-1 Env determines viral susceptibility to IFITM3 impairment of viral infectivity. J Virol 91:e02441-16. https://doi.org/10.1128/JVI.02441-16.
60. Krapp C, Hotter D, Gawanbacht A, McLaren PJ, Kluge SF, Sturzel CM, Mack K, Reith E, Engelhart S, Ciuffi A, Hornung V, Sauter D, Telenti A, Kirchhoff F. 2016. Guanylate binding protein (GBP) 5 is an interferon-inducible inhibitor of HIV-1 infectivity. Cell Host Microbe 19:504–514. https://doi.org/10.1016/j.chom.2016.02.019.
61. Tada T, Zhang Y, Koyama T, Tobiume M, Tsunetsugu-Yokota Y, Yamaoka S, Fujita H, Tokunaga K. 2015. MARCH8 inhibits HIV-1 infection by reducing virion incorporation of envelope glycoproteins. Nat Med 21:1502–1507. https://doi.org/10.1038/nm.3956.
62. Kourtzelis I, Hajishengallis G, Chavakis T. 2020. Phagocytosis of apoptotic cells in resolution of inflammation. Front Immunol 11:553. https://doi.org/10.3389/fimmu.2020.00553.
63. Ongradi J, Ceccherini-Nelli L, Pistello M, Bendinelli M, Szilagyi J. 1990. Different sensitivity to acid reaction of the AIDS virus and virus-producing cells: clinical conclusions. Orv Hetil 131:1959–1964.
64. Sturgill-Koszycki S, Schlesinger PH, Chakraborty P, Haddix PL, Collins HL, Fok AK, Allen RD, Gluck SL, Heuser J, Russell DG. 1994. Lack of acidification in *Mycobacterium* phagosomes produced by exclusion of the vesicular proton-ATPase. Science 263:678–681. https://doi.org/10.1126/science.8303277.
65. Shukla S, Richardson ET, Athman JJ, Shi L, Wearsch PA, McDonald D, Banaei N, Boom WH, Jackson M, Harding CV. 2014. *Mycobacterium tuberculosis* lipoprotein LprG binds lipoarabinomannan and determines its cell envelope localization to control phagolysosomal fusion. PLoS Pathog 10: e1004471. https://doi.org/10.1371/journal.ppat.1004471.
66. Bracq L, Xie M, Lambele M, Vu LT, Matz J, Schmitt A, Delon J, Zhou P, Randriamampita C, Bouchet J, Benichou S. 2017. T cell-macrophage fusion triggers multinucleated giant cell formation for HIV-1 spreading. J Virol 91:e01237-17. https://doi.org/10.1128/JVI.01237-17.
67. Xie M, Leroy H, Mascarau R, Woottum M, Dupont M, Ciccone C, Schmitt A, Raynaud-Messina B, Verollet C, Bouchet J, Bracq L, Benichou S. 2019. Cell-to-cell spreading of HIV-1 in myeloid target cells escapes SAMHD1 restriction. mBio 10:e02457-19. https://doi.org/10.1128/mBio.02457-19.
68. Dargent JL, Lespagnard L, Kornreich A, Hermans P, Clumeck N, Verhest A. 2000. HIV-associated multinucleated giant cells in lymphoid tissue of the Waldeyer's ring: a detailed study. Mod Pathol 13:1293–1299. https://doi.org/10.1038/modpathol.3880237.
69. Geny C, Gherardi R, Boudes P, Lionnet F, Cesaro P, Gray F. 1991. Multifocal multinucleated giant cell myelitis in an AIDS patient. Neuropathol Appl Neurobiol 17:157–162. https://doi.org/10.1111/j.1365-2990.1991.tb00707.x.
70. Vicandi B, Jimenez-Heffernan JA, Lopez-Ferrer P, Patron M, Gamallo C, Colmenero C, Viguer JM. 1999. HIV-1 (p24)-positive multinucleated giant cells in HIV-associated lymphoepithelial lesion of the parotid gland. A report of two cases. Acta Cytol 43:247–251. https://doi.org/10.1159/000330987.
71. Lackner AA, Vogel P, Ramos RA, Kluge JD, Marthas M. 1994. Early events in tissues during infection with pathogenic (SIVmac239) and nonpathogenic (SIVmac1A11) molecular clones of simian immunodeficiency virus. Am J Pathol 145:428–439.
72. Jolly C, Booth NJ, Neil SJD. 2010. Cell-cell spread of human immunodeficiency virus type 1 overcomes tetherin/BST-2-mediated restriction in T cells. J Virol 84:12185–12199. https://doi.org/10.1128/JVI.01447-10.
73. Casartelli N, Sourisseau M, Feldmann J, Guivel-Benhassine F, Mallet A, Marcelin AG, Guatelli J, Schwartz O. 2010. Tetherin restricts productive HIV-1 cell-to-cell transmission. PLoS Pathog 6:e1000955. https://doi.org/10.1371/journal.ppat.1000955.
74. Giese S, Marsh M. 2014. Tetherin can restrict cell-free and cell-cell transmission of HIV from primary macrophages to T cells. PLoS Pathog 10: e1004189. https://doi.org/10.1371/journal.ppat.1004189.
75. Kuhl BD, Sloan RD, Donahue DA, Bar-Magen T, Liang C, Wainberg MA. 2010. Tetherin restricts direct cell-to-cell infection of HIV-1. Retrovirology 7:115. https://doi.org/10.1186/1742-4690-7-115.
76. Dube M, Roy BB, Guiot-Guillain P, Mercier J, Binette J, Leung G, Cohen EA. 2009. Suppression of tetherin-restricting activity upon human immunodeficiency virus type 1 particle release correlates with localization of Vpu in the *trans*-Golgi network. J Virol 83:4574–4590. https://doi.org/10.1128/JVI.01800-08.
77. Bego MG, Cong L, Mack K, Kirchhoff F, Cohen EA. 2016. Differential control of BST2 restriction and plasmacytoid dendritic cell antiviral response by antagonists encoded by HIV-1 group M and O strains. J Virol 90: 10236–10246. https://doi.org/10.1128/JVI.01131-16.
78. Munch J, Rajan D, Rucker E, Wildum S, Adam N, Kirchhoff F. 2005. The role of upstream U3 sequences in HIV-1 replication and $CD4^+$ T cell depletion in human lymphoid tissue *ex vivo*. Virology 341:313–320. https://doi.org/10.1016/j.virol.2005.07.023.
79. Sauter D, Schindler M, Specht A, Landford WN, Munch J, Kim KA, Votteler J, Schubert U, Bibollet-Ruche F, Keele BF, Takehisa J, Ogando Y, Ochsenbauer C, Kappes JC, Ayouba A, Peeters M, Learn GH, Shaw G, Sharp PM, Bieniasz P, Hahn BH, Hatziioannou T, Kirchhoff F. 2009. Tetherin-driven adaptation of

Vpu and Nef function and the evolution of pandemic and nonpandemic HIV-1 strains. Cell Host Microbe 6:409–421. https://doi.org/10.1016/j.chom.2009.10.004.

80. Dave VP, Hajjar F, Dieng MM, Haddad E, Cohen EA. 2013. Efficient BST2 antagonism by Vpu is critical for early HIV-1 dissemination in humanized mice. Retrovirology 10:128. https://doi.org/10.1186/1742-4690-10-128.
81. Sanjana NE, Shalem O, Zhang F. 2014. Improved vectors and genome-wide libraries for CRISPR screening. Nat Methods 11:783–784. https://doi.org/10.1038/nmeth.3047.
82. Ablashi DV, Berneman ZN, Kramarsky B, Whitman J, Jr, Asano Y, Pearson GR. 1995. Human herpesvirus-7 (HHV-7): current status. Clin Diagn Virol 4:1–13. https://doi.org/10.1016/0928-0197(95)00005-S.
83. Platt EJ, Wehrly K, Kuhmann SE, Chesebro B, Kabat D. 1998. Effects of CCR5 and CD4 cell surface concentrations on infections by macrophagetropic isolates of human immunodeficiency virus type 1. J Virol 72:2855–2864. https://doi.org/10.1128/JVI.72.4.2855-2864.1998.
84. Lodge R, Ferreira Barbosa JA, Lombard-Vadnais F, Gilmore JC, Deshiere A, Gosselin A, Wiche Salinas TR, Bego MG, Power C, Routy JP, Ancuta P, Tremblay MJ, Cohen EA. 2017. Host microRNAs-221 and -222 inhibit HIV-1 entry in macrophages by targeting the CD4 viral receptor. Cell Rep 21:141–153. https://doi.org/10.1016/j.celrep.2017.09.030.
85. Richard J, Sindhu S, Pham TN, Belzile JP, Cohen EA. 2010. HIV-1 Vpr up-regulates expression of ligands for the activating NKG2D receptor and promotes NK cell-mediated killing. Blood 115:1354–1363. https://doi.org/10.1182/blood-2009-08-237370.
86. Yuan FF, Mihrshahi S, Fletcher A. 1996. Chemiluminescent enhanced CD47 detection on Western blotting. Electrophoresis 17:219–220. https://doi.org/10.1002/elps.1150170136.